TOWARDS SAMPLING LEAF AREA INDEX USING SMARTPHONES

RICHARD MAKANZA
FEBRUARY, 2015

SUPERVISORS:
Valentijn Venus, ing, MSc
Prof. Dr. W. Wout Verhoef

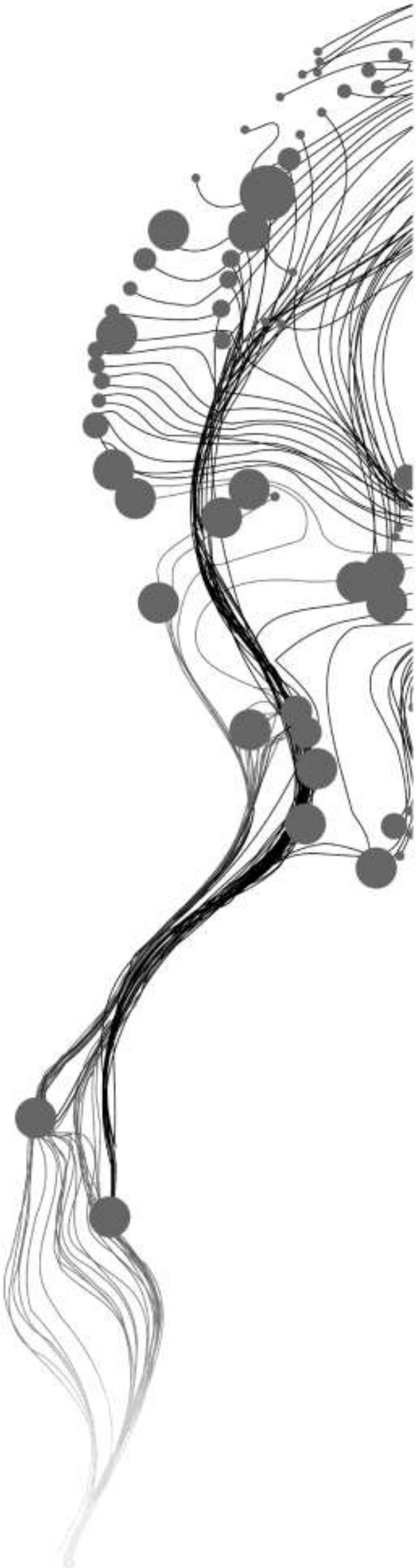

TOWARDS SAMPLING LEAF AREA INDEX USING SMARTPHONES

RICHARD MAKANZA
Enschede, The Netherlands, February, 2015

Thesis submitted to the Faculty of Geo-Information Science and Earth Observation of the University of Twente in partial fulfilment of the requirements for the degree of Master of Science in Geo-information Science and Earth Observation.
Specialization: Natural Resources Management

SUPERVISORS:
Valentijn Venus, ing, MSc
Prof. Dr, W, Wout Verhoef

THESIS ASSESSMENT BOARD:
Prof. Dr. A.K. Skidmore
Dr.ir. B.G.J.S. Sonneveld (External Examiner, SOW-VU)

ABSTRACT

Leaf Area index (LAI) is an important parameter used as input in many biological, ecological and environmental modelling processes. As such , accurate estimation of LAI is a critical step in these process. Estimation of LAI from gap fraction measurements using indirect methods is widely implemented at the viewing zenith angle (VZA)57.5°, when it is independent of the leaf inclination angle. However accurate estimation of this angle remained a problem leading to uncertainties in LAI estimation. The purpose of this study was to evaluate the possibility of improving of LAI estimation by a measuring view zenith angle (VZA) correctly and assessing whether the use of a smartphone motion sensor can be used to improve its measurement. In-order to achieve this the smartphone motion sensor application was tested against a digital inclinometer device to measure the attitude for capturing a maize canopy. The sensitivity of LAI over varying VZA angles was also tested as well as the effect of removal of senescing canopy materials from LAI measurements.

A platform fitted with a smartphone, camera measuring the maize canopy and inclinometer devices was set up. All the devices were corrected to the GPS atomic time at an accuracy less than 0.5 for synchronisation, using time and an identifier of individual VZA observations. The measurements were taken in a video format using the top-looking-down method on a maize canopy approximately 1m tall. Inclinometer VZA readings were also recorded in a video format. A tap was also made before and after rolling the platform to introduce a motion blur on the video and acceleration peaks on the motion sensor that were used to identify the start and end time of each video recording. Synchronisation was performed manually in Total Commander (vs 8.01) software in a three tile graphical user interface (GUI), with excel data from smartphone as reference. Image classification was performed using object based image analysis method (OBIA) in eCognition and gap fraction extraction in CAN-EYE software. Validation of the classification was performed using an independent student t-test. A ordinary least square regression model was used to test the relationship between the smartphone and inclinometer VZA measurements, as well as the sensitivity of LAI to the variation in the VZA. The uncertainty of LAI due to variation in the VZA were compared to a theoretical root mean square error (RMSE) of 5% reported by Baret, *et al.*, (2010). Furthermore a student t-test was also used to assess the effect of removal of senescing canopy material on LAI measurements.

The smartphone and inclinometer VZA measurements were strongly correlated (R^2=0.998, RMSE=1.081). We therefore failed to reject the null hypothesis and concluded that the two measurements were different from each other. Conversely there was a weak correlation between LAI measurements and VZA-Error for both smartphone (R^2 =0.0247, RMSE = 0.96). However RMSE for the sensitivity analysis was not significantly different from the theoretical one of 5%. Furthermore the removal of senescence significantly ($P>0.05$) reduce the LAI measurements assuming equality of variance (($P>0.05$) for both smartphone and inclinometer readings. In conclusion it was observed that even thought there are some errors associated with obtaining the VZA correctly, these errors do not cause significant errors in the estimation of LAI. However senescing canopy materials can significantly affect LAI estimation from gap fraction measurements.

ACKNOWLEDGEMENTS

My heartfelt pleasure to extend my appreciation to Valentijn Venus for the opportunity he granted me to explore an exciting, yet challenging research study. It was worthwhile and I feel have learnt a lot. More importantly Valentijn, you have been so patient and understanding, yet relentlessly guiding me to a successful completion of my study. I was challenged by your critical thinking and attention to detail, yet inspired your passion and enthusia for new technology. In short, you have changed the world around me. To Prof. Wout, I have been humbled to have you as my second supervisor. Yours was not just only supervision, but also fatherly guidance. Every time you were in the office, you were always ready to assist despite a busy schedule. Every resource at your disposal, you were ready to make it available for the success of my thesis. To both of you I say thank you.

The success of my thesis could not have been possible without mentioning Harry and Bernadette. At the point when the hope to carry out my field work was fading. You kindly allowed me to carry out my field work at your farm until successful completion of my data collection. I am humbled to say to Bernadette, you are so special. I vividly remember your hospitality, in the cold rainy weather, you gave me shelter and even transport to go to the bus stop. Above all, I really enjoyed the coffee time we had together with Harry.

To my classmates and friends at ITC, you have made my learning environment easy. Every challenge I faced you were ready to help. Firstly to Fang, thank you for your assistance to prepare for the field work, companionship during the field work and ideas too. My colleagues from Zimbabwe and SADC, you made me feel at home. My colleagues from Kenya, thank you for your support during the preparation of my field work.

Willem, I really appreciate your assistance in the development of the app. More importantly for sparing your time to share your ideas and show me how it works. Your patience too, to make sure that everything is working for the success of my thesis. Watse thanks for your help in fixing the platform and organising field work equipment too.

My special thanks also goes to the ITC and NUFFIC, for granting me the opportunity to study my MSc degree through academic and financial support respectively. The skills I have acquired will go long way in making Africa a better place to be. I am also indebted to my bosses at Ministry of Agriculture for providing every support and time for me to come and study here in the Netherlands.

To my loving wife Tsitsi. You allowed me to go way and patiently waited for me, you brought comfort in hard times; prayed and encouraged me. I love you so much. My two parents your continual support and encouragement has seen me this far.

To God the Almighty be all the glory!!!!

TABLE OF CONTENTS

LIST OF FIGURES

LIST OF TABLES

LIST OF APPENDICES

1. INTRODUCTION

1.1. Background

The leaf is considered as one of the most important part of vegetation canopies due to its functional role in both biochemical and biophysical plant processes. Firstly, leaves are organs of exchange of materials between the plant and the atmosphere such as radiation energy, water, carbon dioxide and oxygen. The outward movement of water from the plant into the atmosphere enhances uptake of more water and nutrients by the plant roots from the soil environment. These materials, are fundamental inputs for photosynthesis, a process that drives plant growth and development. Secondly, the leaf exchange processes also naturally modifies the plant micro-environment by changing the air quality and temperature which enhances biodiversity. Hence leaf measurements play an important role in understanding temporal and spatial states of the plant and its environment.

Leaf area index (LAI) is a dimensionless variable used to quantify the amount of leaves in vegetation canopies. According to Watson (1947), it is defined as "the total one-sided surface area of photosynthetically active leaf tissue per unit horizontal ground surface area expressed in m^2/m^2". LAI is used an input parameter in modelling of ecological, environmental, climate and crop growth processes. Therefore, accurate estimation of LAI of vegetation canopies is a critical step in these modelling processes.

Different approaches employing direct and indirect methods can be used to estimate LAI. The former, which involves manual measurement of individual canopy elements using planimeters is time consuming and laborious. Hence it is applicable to small scale LAI measurements, and is normally used as reference to the latter. In addition direct methods are destructive in nature, and therefore cannot be used for trees which can take longer time to replace. Conversely, indirect methods which measures LAI non-destructively from radiation transmission through the canopy, captured as gap fractions, are faster and less laborious. Gap fraction is defined as "the size of horizontal ground surface area as seen from above the canopy or size of the sky area as seen from below the canopy in the zenith and azimuth directions. (Bréda, 2003a; Weiss, *et al.* 2004b) A wide range of instruments used to measure gap fraction include single detector sensors e.g. TRAC and DEMON; ceptometers: SUNSCUN, ACCUPAR and Decagon (Chen & Cihlar, 1995) and multidirectional sensors Hemispherical photography (Demarez *et al.*, 2008) and LAI2000 (Nackaerts *et al.*, 2000). In addition, recently Baret *et al.*, (2010) and Liu *et al.* (2010), reported on the use of digital photography with restricted field of view around zenith view angle 57.5°. Single sensor can be used both under direct or diffuse light conditions while multidirectional sensors produce better results under diffuse light conditions (Baret *et al.*, 2010). These methods are capable of capturing measurements from the whole canopy or a group of canopies instantaneously, and hence can be used for larger scales. For this reason, indirect methods have become more popular than direct methods, and are widely used to measure LAI.

LAI can be estimated from gap fraction measurements using an exponential Poisson distribution model, assuming a random distribution of leaves within the canopy architecture. This assumption is more theoretical than reality, for most vegetation canopies, are naturally aggregated and dispersed at various scales i.e. shoot, branches, plant in the case of forest and landscape level in row crops (Weiss *et al.*, 2004a). Hence LAI derived based on this assumption is called effective leaf area index (LAI_{eff}). To account for this non-random distribution of leaves, Nilson (1971) introduced a clumping index (λ_0), which modified the Poisson model. As a result a new term LAI_{eff}, was defined as a function of clumping and true leaf area index (LAI_{true})(N.J. J. Bréda, 2003). Furthermore, gap fraction measurements are also influenced by a view zenith direction, assuming an isotropic azimuth angle. Gap fraction is commonly measured at 57.5 view zenith angle when LAI estimates are in insensitive to leaf angle distribution (Wilson, 1960). When this directional configuration is perpendicular to the row, in the case of row crops, clumping is also minimized (Baret *et al.*, 2010). However the controversy of LAI_{true} estimation from gap fraction measurements is still an on ongoing debate with several issues being addressed. The measurement of gap fraction does not only account for green leaves, but also for stems, branches and flower parts which in some cases are also green as it is with row crops. In addition, senescing vegetation elements are also an important factor, that influences gap fraction measurements. Hence LAI can be referred to plant area index (PAI), when all vegetation elements are included or green area index (GAI), when only green parts are taken into account. Since the essence of LAI measurements is to quantify the green parts of the leaf, GAI has been viewed to be an alternative to LAI and PAI. Baret *et al.*, 2010 and Liu, 2010 have reported on the estimation of GAI from gap fraction using digital photography.

Smart phones are increasingly becoming popular in digital photography due to their versatile usage. They are equipped with high quality camera sensors, increasing memory and fast computational capabilities (Havlik & Schimak, 2014). In addition, their sizes featuring 3.5 to 4.3 inch LCD touch screens renders them convenience of portability and functionality. Most users also enjoy the convenience that smartphones offers when they take photographs and instantly store them in cloud databases or post them on social networks such as instagram or facebook (Digital Imaging Reporter, 2011). These functionalities have made them unique and more attractive to their users than dedicated digital cameras. Enhanced by gapless wireless network environments, their usage have exponentially increased resulting their ready availability even at low costs (Ebay, 2014). The question of picture resolution would appear pertinent yet today`s smartphone devices boast near professional performance with minimum of 5 MP up to 13 MP in many modern cell phones. Although their usage seems to be more pronounced in the social networks, it is indeed growing in the scientific fields, as indicated by development of many applications (apps.) for research and development purposes (Cellina *et al.*, 2013, Confalonieri *et al.*, 2013, Francone,*et al.* 2014, Havlik & Schimak, 2014).

More interestingly, smart phones have motion sensors, supported by an android platform that can enhance their photographic functionalities. These inbuilt hardware are pertinent to accurate estimation of view zenith angle (VZA) of the device whilst taking photographs. This gives them an edge over digital cameras which requires a detached angle gauge alongside the device to measure its VZA. Smartphone motion sensors include accelerometers, which provides gravity vector in relation to the phone's body; magnetometer, which gives a direction with respect to the magnetic north and gyroscope which provides angular rotation speeds to all the three sensors. The phone's motion such as the yaw, pitch and roll which is usually a direct response of the user input, are measured by accelerometers and gyroscopes, while its position by magnetometers. However, the output of these sensors are inaccurate when they are used individually due to noisy orientation in accelerometer and magnetometer measurements, and gyro-drift in gyroscopes. Gyro drift occurs when gyroscopes accumulate errors over time resulting in a general shift of angular rotation speed measurements. In-order to avoid these inaccuracies, sensors can be fused together via complimentary filters with a low pass filtering for accelerometer and magnetometer, and a high pass filtering for gyroscopes (Android Developers). This ensures more accurate monitoring of the device`s position and movement. In a recent generic app, Pocket LAI (App-G and App-L) implementing accelerometer and magnetometer sensor data only, an attempt was made to measure gap fraction at VZA 57.5^0, from both the top and bottom of the canopy directional configurations. Unfortunately, the precise estimation of the angle remains a challenge leading to the uncertainty in the estimation of LAI. Novel gyroscope sensor fusion via a complementary filter with acceleration and magnetic sensor data could help improve prospects for sampling LAI by mobile devices.

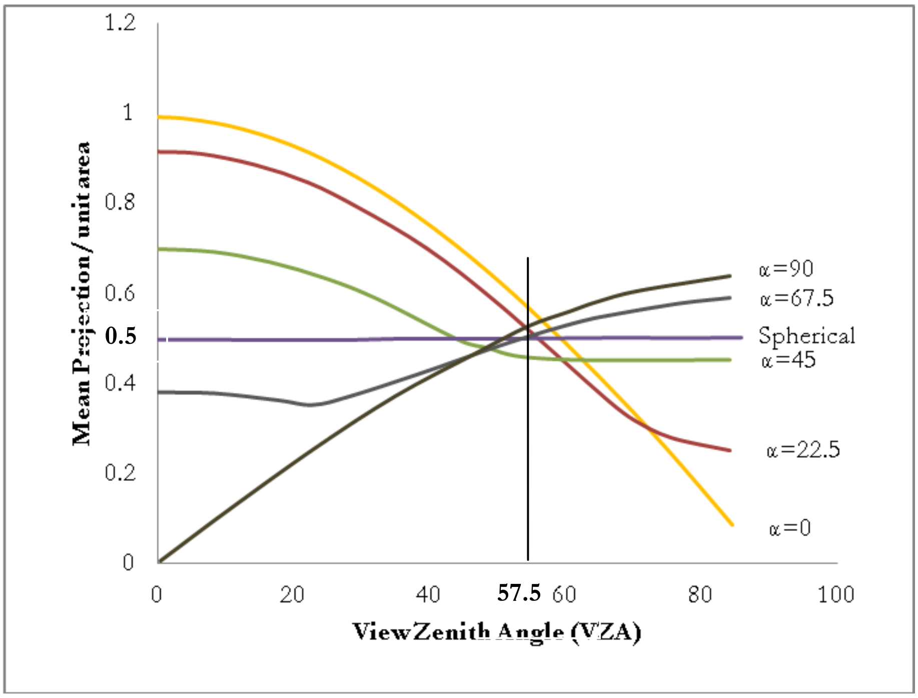

Figure 2. Mean projections for different leaf distributions in the VZA direction.

(where α= average leaf inclination angle); source: (Chen & Black, 1991)

1.2. Research Problem

The Wilson (1960)'s, inclined point quadrant method which demonstrates relative independence to leaf inclination angle of LAI estimates taken at VZA 57.5°, is a widely accepted concept used to extract gap fraction measurements. As illustrated in (**figure 1)** above, the mean projection functions of unit foliage (G-function) on a plane normal to the direction of the beam of light converge at this VZA, assuming a spherical distribution of leaves. The G-function value at this point of convergence is 0.5. However estimation of the VZA 57.5° still remains challenging leading to uncertainties in the estimation of LAI estimation. For instance, the use of monopod and tripod stands have problems in estimation of the VZA 57.5° due to verticality of stands and observer errors in reading the inclinometer scale. These problems are normally caused by field related factors like evenness of the ground and operational height for taking photographs. Furthermore, an attempt to use smartphone sensors to estimate the VZA 57.5° was made in a recent generic app: Pocket LAI (App-G and App-L), implementing accelerometer and magnetometer sensor data only in both downward looking and upward looking directional configurations. Unfortunately, the attitude measurements from these sensors alone are erroneous due to noisy orientation (Android Developers). Hence the precise estimation of the VZA 57.5° using these smartphone apps. is still problematic, leading to uncertainty in LAI measurements. The variation of the VZA around the 57.5° may lead to an estimation of the G-function above or below G=0.5 (**figure 1**). Since the range of G is small, from 0.3-0.8 for measured canopies (Myneni *et al.*, 1989), the sensitivity of LAI due to the VZA uncertainties has not been quantified.

The ability to separate green from senescing canopy materials is also another milestone towards accurate estimation of LAI from gap fraction using photographic methods. Senescing canopy materials reduces the size of gaps through which light travels within the canopy leading to an overestimation of LAI. Conversely, absence of senescing canopy material leads to increase in gaps within the canopy, also leading to a decrease in LAI estimation. Hence the more the amount of senescing materials the greater the impact on LAI estimation. However, in most studies assumptions of uniformly green canopies are always made through visual assessment of the field, when measuring gap fraction using photographic methods. Despite the crop stage, these assumptions may not conform to realities of the state of plants as a result of spatial and temporal variability of biophysical factors in a field causing stress on crops and leading to senescence. The levels of stress may vary from wilting to pigment colour change and plant death as an extreme case. Wilting and colour which are highly temporal in nature, may result in increased gaps between plants leading to underestimation in LAI. It is however important to note that reduction in the green pigmentation of the plant leads to increased gap fraction since LAI_{true} estimation accounts for the green parts of the canopy only. This is normally called green gap fraction. Nevertheless, cell death is normally irreversible and cause a permanent change in the gap fraction. In addition stress may also result in change in the plant stamina, which directly influences the size of canopy elements: stem, leaf and flower. These directly influences gap fraction. As a result, variation of plant state and condition in space and time may lead to uncertainties in LAI estimations.

LAI estimation from gap fraction measurements is normally performed using the Poisson distribution model or the adjusted form of the model, known as the Markov model to estimate LAI_{eff} or LAI_{true} respectively. The difference between the two is the accounting for clumping index (λ_o) in the latter. However the uncertainties of LAI estimation from gap fraction measurements have only been quantified in a theoretical study using the Poisson model when the variation around the VZA 57.5^o was less than 2^o (Baret *et al.*, 2010). In this case, clumping and senescing canopy elements were not accounted for in the computation of the uncertainty. Furthermore, in a parallel study by the same author, a field of view of around $\pm$5^o around the VZA 57.5^o was used. Although this method assumes that negative and positive errors cancels each other, the uncertainties of in this assumption on LAI is known. This is because the magnitude of either positive or negative errors around the VZA 57.5^o may not be equally follow an obvious pattern. In order to understand these uncertainties in LAI estimation, measurements should be carried on wider VZA range, 50^o-60^o, when the G-function is close to 0.5 (Myneni et al., 1989; Ross, 1981) and accounting clumping and senescing canopy elements.

1.3. Objectives

1.3.1. Overall Objective

The purpose of this study was to evaluate the possibility of improving of LAI estimation by measuring VZA correctly and assessing whether the use of a smartphone motion sensor can improve in the its measurement.

1.3.2. Specific objectives

Objective 1: To test the capability of motion sensor fusion technique to estimate the VZA.

Objective 2: To quantify the uncertainties of LAI estimates.

Objective 3: To evaluate the effect of removal of senescing canopy material on LAI estimation.

1.4. Research Hypothesis

1.4.1. Hypothesis 1

Ho: The root mean square error (rmse) in determining the camera's attitude, notably the (VZA), is greater than zero at 95% confidence interval (rmse>0).

H1: The root mean square in determining the VZA is equal to zero at 95% confidence interval. (rmse = 0).

1.4.2. Hypothesis 2

H0: The sensitivity of LAI estimates to errors in the VZA is not more than 5% [1]

H1: The sensitivity of LAI estimates to errors in the VZA is more than 5%[1]

1.4.3. Hypothesis 3

H0: There is no significant decrease in LAI estimates due to the removal of senescing canopy material

H1: There is significant decrease in LAI estimates due to the removal of senescing canopy material

1.5. Research questions

1. What is the success rate of smartphone to estimate zenith view angle?

2.1 Are the uncertainties of LAI estimates greater than 5%?
2.2 What is the sensitivity of LAI at non-steady view zenith angle?

3. Is there a significant decrease in LAI due to senescing canopy material?

1.6. Research Assumptions

1. For this research, which focuses on the technical aspects of sampling LAI by smartphone, operator-related errors are assumed.
2. Clumping index was implicitly accounted for in LAI measurements from CAN-EYE software.
3. Digital photographs taken by a normal camera are assumed to be similar with the ones from a smartphone.
4. Radiation transmission through the canopy assumes: black foliage (under 490nm); foliage elements smaller than area of view of the sensor; foliage is azimuthally randomly oriented. Although no real canopy exactly conforms to these assumptions the model still works (Weiss *et al.*, 2004).

1.7. Definition of terms

Sensitivity: refers to the degree of responsiveness of an output variable (LAI_{true}) to change in the input variable (VZA).
Uncertainty: refers lack or limited of knowledge about occurrence or state of an event, whereby a probability can be assigned to it as a possible measurement.

[1]5% is the root mean square error (RMSE) when clumping and non-green elements where not accounted for (Baret et al., 2010)

2. MATERIALS AND METHODS

2.1. LAI and Gap Fraction Theory

2.1.1. Definition of LAI

LAI is the integration of leaf area density per unit canopy volume *l* (m^2/m^3) and canopy height *h* (m), as follows.

$$LAI_{true} = \int_0^H \boldsymbol{I}(h)dh \qquad \textbf{Eq. 1}$$

Acronym	Definition
*LAI_{true}	The area index (m^2/m^2) of all the green parts of the canopy including: leaves, stems e.t.c.
*LAI_{eff}	The area index (m^2/m^2) after accounting for clumping.
LAI_{canopy}	The total area index (m^2/m^2) of the canopy inclusive of green and non-green.
LAI_{gl}	The total area index for green leaves only
LAI_{gs}	The total area index for stem only

Table 1 LAI definitions used in this study.

** Assumption of clumping applies*

2.1.2. Gap fraction Theory

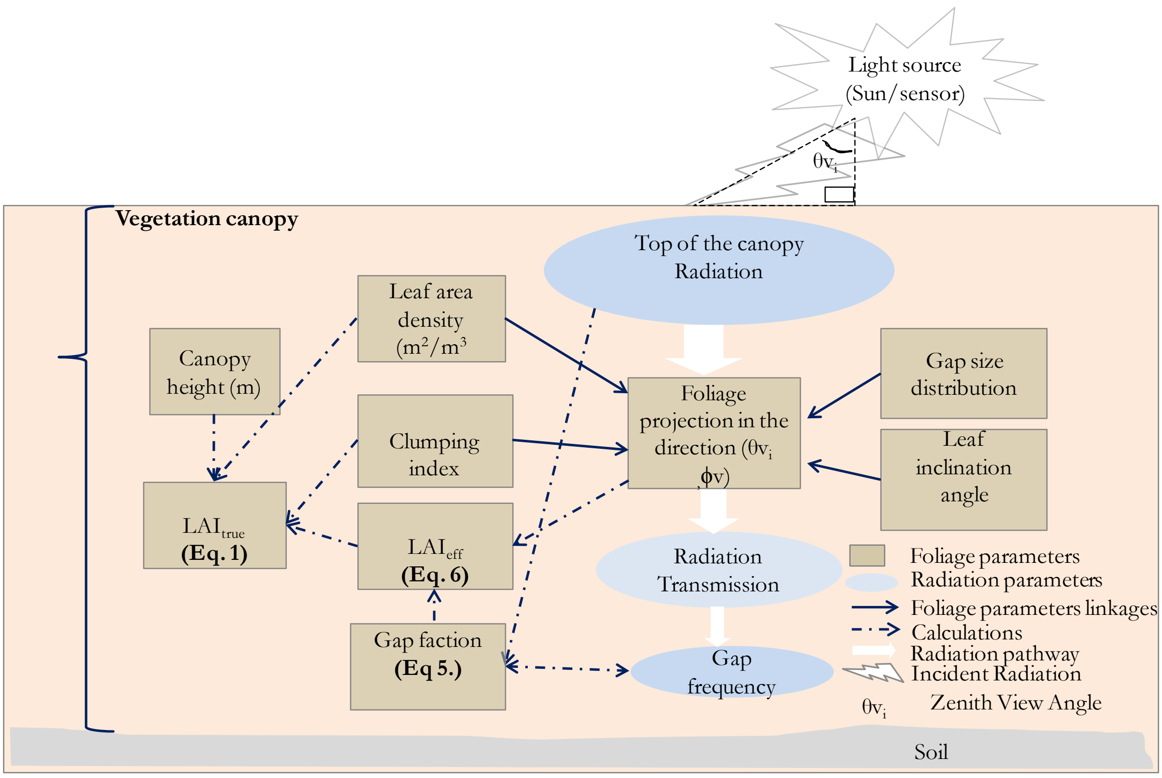

Figure 3. The gap fraction conceptual diagram.

The probability of a beam of light passing through the canopy and coming into contact with vegetative parts in the zenith view direction (θ_v) assuming an isotropic azimuth angle(φ_v), and at a canopy height (H), is given as mean number of contacts [$N(H, \theta_v, \varphi_v)$]as follows:

$$N(H, \theta_v, \varphi_v) \int_0^H \frac{G(H, \theta_v, \varphi_v) I(h)}{\cos\theta_v dh} \quad \textbf{Eq. 2}$$

where $G(\theta_v, \varphi_v)$ is the mean projection of a unit foliage area in the direction (θ_v, φ_v) and the inverse of cos(θv) is the path length through which radiation travels. When $G(\theta_v, \varphi_v)$ and leaf area density at a particular height $l(h)$ are independent of canopy height (H), then **Eq. 2**. simplifies to:

$$N(\theta_v, \varphi_v) = \frac{G(\theta_v, \varphi_v) l(h)}{Cos\theta_v dh} = \frac{G(\theta_v, \varphi_v) LAI_{true}}{Cos\theta_v} \quad \textbf{Eq. 3}$$

The fraction of light passing through the canopy to horizontal reference surface, is exponentially related to contact frequency assuming a random turbid medium, according to the Lambertian law as follows:

$$P_0(\theta_v, \varphi_v) = e^{-N(\theta_v, \varphi_v)} = e^{-\frac{G(\theta_v, \varphi_v) LAI_{eff}}{Cos\theta_v}} \quad \text{(Warren , 1959)} \quad \textbf{Eq 4}$$

where $P_0(\theta_v, \varphi_v)$ is the gap fraction.

When non-random distribution of leaves in infinite layers within a canopy is assumed the Markov model which accounts for conditional probability of radiation transmission within a canopy assuming zero or one contact per layer is used (Weiss *et al.*, 2004). The probability of contact in a layer depends on whether there has been a contact in the previous layer (Jonckheere *et al.*, 2004). Therefore, the Poisson distribution model is modified as follows:

$$P(\theta_v, \varphi_v) = \frac{-\lambda_0 G(\theta_v, \varphi_v) LAI_{true}}{Cos\theta_v} \quad \text{(Nilson, 1971)} \quad \textbf{Eq 5}$$

where $\lambda_0$is clumping index: the degree of aggregation or dispersion of leaves in infinite layers within a canopy, where $(\lambda_0 < 1)$ for clumped canopies and $(\lambda_0 > 1)$ for regular canopies.

2.1.3. From Gap Fraction to Effective LAI (LAI_{eff})

LAI_{eff} is a function of clumping index and LAI_{true}, hence is given by inversion of **(Eq.5)** as follows:

$$LAI_{eff} = \lambda_0\, LAI_{true} = \frac{-cos\theta_v \ln P_o(\theta_v, \varphi_v)}{G(\theta_v, \varphi_v)} \quad \textbf{Eq 6}$$

There are two ways to derive LAI_{eff}, given that both gap fraction and clumping are known. Firstly by solving **Eq. 6** simultaneously for the projection function; $G(\theta_v, \varphi_v)$, given that gap fractions are taken at a range zenith view angles. Secondly, by computing the slope of the regression of LAI_{true} . According to Nilson (1971) and Ross (1981), extinction coefficient $k(\theta)_v$, is a function of path length $(cos\theta_v{}^{-1})$) to be travelled by radiation and mean projection of unit foliage area $G(\theta_v, \varphi_v)$, in the zenith direction on a plane perpendicular to the beam of light and is given by:

$$k(\theta)_v = \frac{-G(\theta_v, \varphi_v)}{cos(\theta_v)} \quad \textbf{Eq 7}$$

Hence, by inversion of Eq. 6., $k(\theta)_v$ is the slope of a regression of LAI_{true} and the value from the left side when gap fraction and clumping are known and can presented as follows:

$$\frac{-\ln P_o(\theta_v,\varphi_v)}{\lambda_o} = k(\theta)_v\, LAI_{true} \qquad \textbf{Eq. 8}$$

2.2. Study Area

Data was collected data from a late-planted maize field at Rossum area in the Netherlands on the 26th and 27th of October 2014. At this time, the crop was at early flowering to maturity stage, hence varying levels of senescence. Although the crop was planted on the same day, 15th June 2014, it exhibited different heights due to varying soil types and water logging across the field. As a result three major height categories: short (<1 m), medium (1-1.5m) and tall (above 1.5m) characterized the field. The short maize category with approximately an area of 2000m²,was subject to a combination of stress factors as a result of poorly drained sandy loam soils. As the soil type gradient changed from sandy loam to black clays, plant height also changed from short through medium to tall respectively. These three plant height categories constituted homogenous units within the same maize field. However, in this study, only the short maize category was considered for data collection so that the top-looking-down method can used because it captures the whole canopy with rectilinear photographs.

Figure 4. The field from where data was collected.

2.3. Data collection Methods

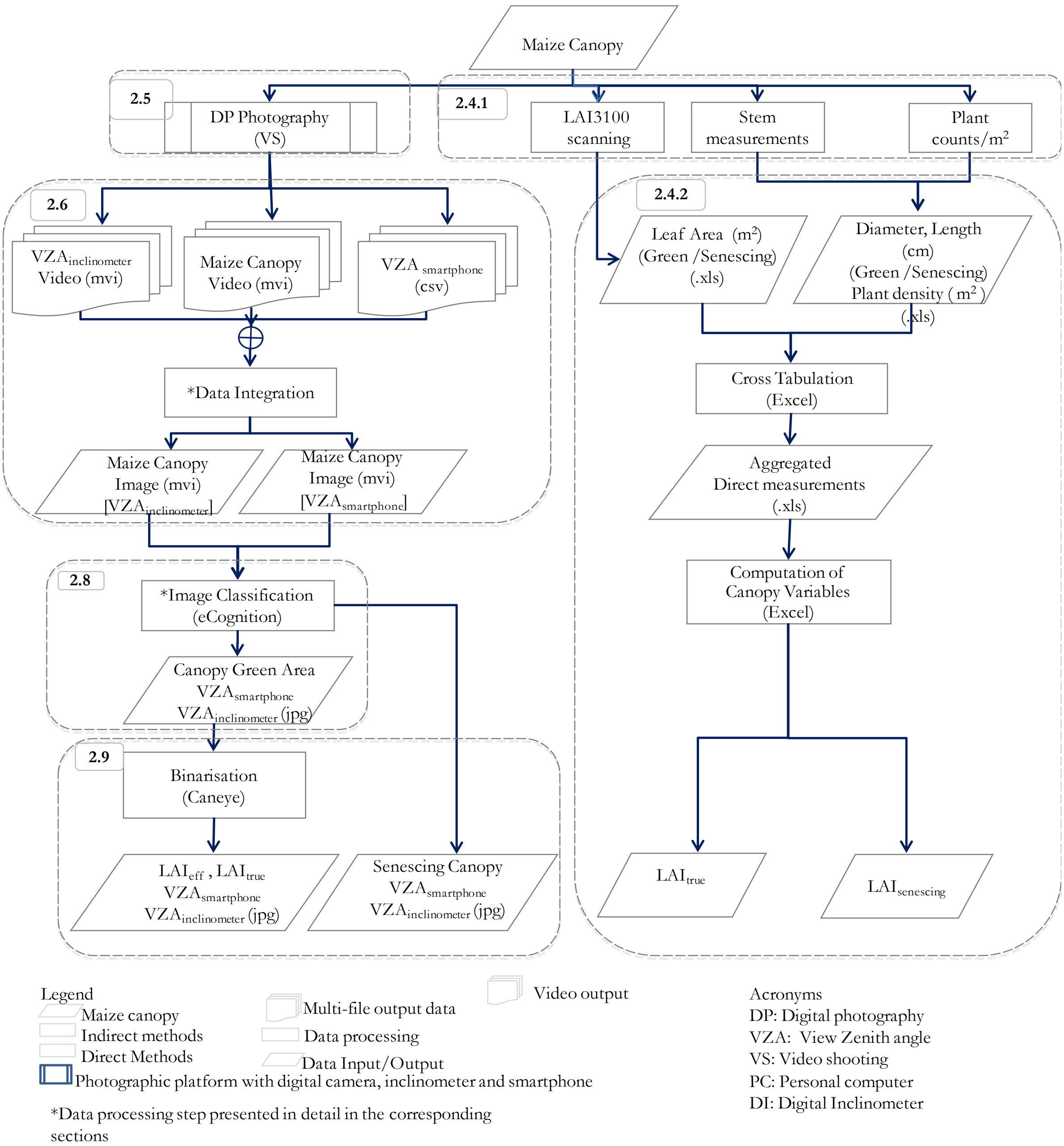

Figure 5 The flow chart of methods used to collect and process data.

2.4. Direct measurements

2.4.1. Field Measurements

A systematic point sampling approach was used to sample 50 plots of 6 x 4 m^2 size. Three plants were selected per plot at 2m intervals for measurement of leaf area, 1/2 stem diameter and, stem length. Leaf area measurements were performed using a LI3000 portable leaf area planimeter. The leaves were scanned non-destructively and, cumulative green and non-green area were recorded separately per plant. Similarly, length and diameter of stem was measured using a tape measure and pair of vernier callipers respectively from the same plants. Plant stem length measurements were taken from the foot of the stem to the tip of the tassel, while 1/2 stem diameter just above the ear. However, tassel structure was assumed to be a single unit of the stem with all its spikelets', hence stem measurements were done inclusively. In addition to plant canopy measurements, plant density was also measured by counting number of plants in 1m transects. Three transects were selected diagonally across the plot. An average plant density was calculated and recorded per plot.

2.4.2. Data Processing

All the direct measurements were recorded and aggregated to plot level in excel to compute the desired canopy variables. On one hand green leaves index (LAI_{gl}) was calculated as a product of plant density (m^2) and average green leaf area (m^2), therefore exclusive of non-green leaf area. On the other hand, LAI_{gs} (m^2/m^2) was computed from stem lengths and 1/2 stem diameter (m^2). LAI_{true} was computed from the summation of LAI_{gl} and LAI_{gs} (m^2/m^2). Similarly senescence was also computed by aggregating stem and leaf area indexes. The equation below were illustrated using LAI_{true} calculations.

$$LAI_{gl} = \frac{Area\ (cm) * D\ (plants/\ m^{-2}\ )}{10\ 000} \qquad LAI_{gs} = \frac{{}^{1}/_{2} sd(cm) * sl(cm)}{10\ 000} \qquad \textbf{Eq 12-14}$$

$$LAI_{true} = LAI_{gl} + LAI_{gs}$$

where D is plant density in, SA is stem area, , sd is stem diameter and , sl is stem length

2.5. In-direct Measurements

2.5.1. Smartphone motion sensor

The smartphone was equipped with a motion sensor application to provide angle data for measurement of canopy VZA at an average accuracy of at least 1.1milliseconds (ms). Angle information was provided at the rate 25 observations per second and at 40 (ms) intervals between observations. Data was downloaded and accessed in a tabular form with variables observing the attitude of the smartphone i.e. pitch (VZA), acceleration and timestamp as column names. The timestamp recorded the lapse of time during the iterations while the start time was given as part of the file name code for easy identification as given below.

	E	F	G	H
1	Timestamp(ms)	Acceleration	Y-roll (VZA)	Gyro
2	0.063000	0.227750	50.750295	0.003084
3	0.082000	0.583940	51.297071	0.001987
4	0.140000	0.627663	51.736991	0.002134
5	0.166000	-1.181916	52.086923	0.003214
6	0.214000	1.453225	52.469126	0.002480

Figure 6 a) Smartphone attitude (Y-roll) used as VZA and **b)** the data template .

2.5.2. Digital Photography

Maize canopy was captured under cloudy conditions using a digital Canon EOS mark II 5D camera fitted with a normal lens. A video footage was shot from top looking downwards at the highest possible resolution of (5616 x 3744 pixels), normal exposure, and shortest focal length 35mm, as advised by Liu *et al.*, (2010). Furthermore the frame rate was set at 24 frames per second (fps) for efficient storage space utilization. A digital inclinometer device and smartphone motion sensor were used to record the VZA at which the canopy was captured. The inclinometer was paired with another camera device (Olympus Stylus tough, 8010), to record its VZA. Nevertheless the smartphone automatically recorded VZA data from the app and store it in the phone memory.

In order to harmonize measurements from all the equipments three steps were followed. Firstly a high level of synchronicity of the canopy and VZA measurements on the same time scale was a requirement. The device time of the instruments were set to the GPS atomic clock time via GPS atomic clock application at accuracy of less than 0.5 seconds. Time synchronization was always checked every time the devices were switched ON either from a sleep or a complete power-OFF mode. Secondly, the three cameras and smartphone were set up on an aluminium platform fitted on a flexible and stable tripod head. The tripod head was wide enough to balance the platform and had a handle long enough to ensure smooth leverage of the platform weight. Lastly, the $VZA_{smartphone}$ and $VZA_{inclinometer}$ were set at zero before the measurements were taken.

At this point the platform was raised 1m above the canopy in the perpendicular direction to the rows of maize canopy. A series of routine steps were performed at each point measurement. Firstly, the devices were switched on in series, followed by a small tap to vibrate the platform introducing a momentary motion blur on the video recorded by the devices. Secondly the platform was then tilted forth and back from top-looking-downwards direction to capture maize canopy video footage until VZA between 50° and 60° were recorded by the two angle devices. Thirdly another tap was made to signal the end of one point measurement. Lastly but not least, all the devices were switched again in series. In essence, two canopy measurements were taken at the same time per sampling point i.e. canopy at $VZA_{smartphone}$ and canopy at $VZA_{inclinometer}$. Although the measurements were taken at the same time, the attitude of the angle devices were assumed to be reading differently as the platform was inclined back and forth.

a) b)

Figure 6 a) An aluminium platform setup **b)** routine video recording steps.
(2) *tripod head* ***(3)*** *android smartphone* ***(4)*** *EOS digital camera* ***(5)*** *digital inclinometer* ***(6)*** *Data Integration*

2.6. Data integration

The VZA at which each maize canopy frame in a video was taken was estimated by synchronizing each video frame with event angles from $VZA_{inclinometer}$ and $VZA_{smartphone}$ on the same time scale. Integration of canopy data and its VZA was done manually Total commander. The software has a graphical user interface (GUI) with tiled windows for data input, visualization and output in one graphical display A pair of data sets were synchronised at a time.

Canopy and $VZA_{inclinometer}$ video data sets were first converted into *.jpg* frames at 24 *fps* and 30 *fps* using Free Video to JPG converter software (v 5.0.5.4 build 1215) (DVDVideoSoft). Frames for each video were automatically numbered from the first frame to the last and also stored in separate folders through the software internal automation during the conversion process. The frame number were considered an equivalent of the frame index numbers of the video frames because they processed using the same recording frame rate.

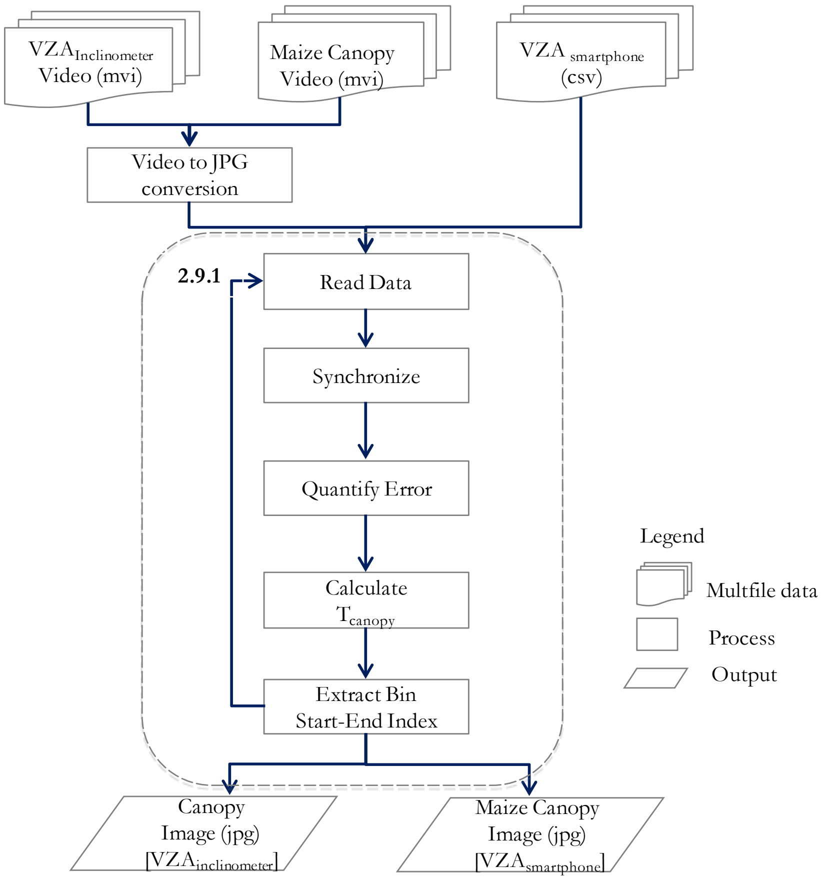

Figure 7: Data integration step

2.6.1. Data Synchronization

The VZA of a particular canopy frame was estimated using a specific time at which the frame was taken. A particular frame in a video was identified by a frame index code which defined a specific position of the frame in a video footage. The $VZA_{smartphone}$ data was used as reference to estimate the maize canopy and $VZA_{inclinometer}$ data. Furthermore, acceleration data from the smartphone motion sensor was also included to identify the imposed platform tap with its characteristic high peaks. Firstly, specific recording time for each $VZA_{smartphone}$, was given by **Eq. 14** where (t) is the elapsed time from the initial time (T_0).

$$T_{VZA_{smartphone}} = T_0 + t \qquad \textbf{Eq 14.}$$

Secondly the offset or error (E) between the start time $T_{0(VZAsmartphone)}$ and $T_{0(Canopy)}$ was computed through **Eq. 15.**

$$E = T_{(Canopy)} - T_{oVZA_{smartphone}} \qquad \textbf{Eq 15.}$$

Thirdly, T_{Canopy} for each canopy frame was then calculated with respect to the camera frame rate (FR) by **Eq 16.** below.

$$T_{Canopy} = T_{VZA_{smartphone}} + E * FR \qquad \textbf{Eq 16.}$$

At this point, an excel sheet showing T_{Canopy} for each frame and the corresponding $T_{(VZAsmartphone)}$ for each $VZA_{smartphone}$, were opened in the same PC window interface with Total commander. The angles between 50^0-60^0 were displayed by hiding unwanted data, and the corresponding index files were identified. Canopy images were identified with their angles through binning, where range of angles were deliberately defined. All images within a bin were selected and stored in their respective bin folders. In this way, the uncertainties introduced by the inconsistency in the recording rate of either $VZA_{smartphone}$ or Canopy frames data were minimized by selecting the central video frames from each bin folder for processing.

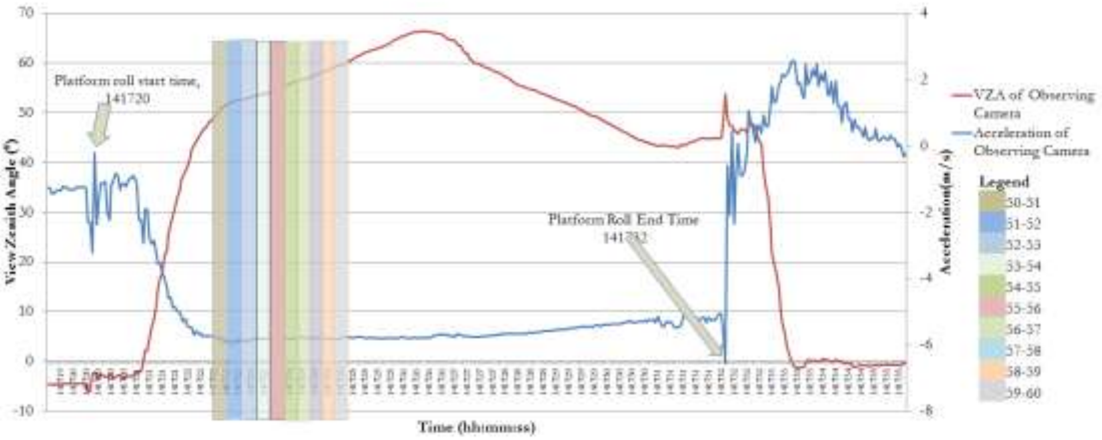

Figure 8. The binning process of frames in Total commander

Elapsed Time (sec)	$VZA_{smartphone}$ (float)	VZA_{Bins} (integer)	Canopy Frames (integers)	$VZA\text{-}Frames_{Inclinometer}$ (integer)
4.228	50	1		
4.258	50.1	1		
4.328	50.17913016	2		
4.361	50.3676191	2		
4.493	51.37721698	3		
4.525	51.46527482	3		
4.561	51.64854488	3		
		....		
6.286	58.08530301	10		
6.329	58.25929859	10		

Figure 9. Reference excel data from $VZA_{smartphone}$.

2.7. Data File Management

The data management system implemented in manual and matlab is worthwhile to elaborate because of the volumes of data that was managed. A three tile GUI was created in Total commander via the "switch through tree panel" option which enables creation of a customized GUI. Hence the input file directory was opened in the left window and files were dragged into the centre visualization window, where images were identified by their index numbers. A group images for a particular bin were then dragged into the right window where the output directory was located. The scroll bars in all the windows facilitated quick navigation to file directories and images during synchronization. Other tools like "multi-renaming" helped to increase the efficiency on processing of the images. In this way, thousands of images were quickly processed in a short space of time. The syntax below show pathways the out file directories

Output File:[camera_vendor]_[dd]/[mm]/[yyyy]_[hh:mm:ss]_[angle

Example: ...\"OLYMP_12-10-2014_09432906_51.53.jpg"

Output Directory: [Drive]_[Database]_[Canopy-strata]_[Photographic-Method]_[storage-destination]_[Motion-sensor]_[Bin]_[PlotID]_[ReplicateID]

Example: H:\Research_data\TL\DHP\Data_out\accgy\ 50-51\plt_1\Rep1\...

2.8. Image Classification

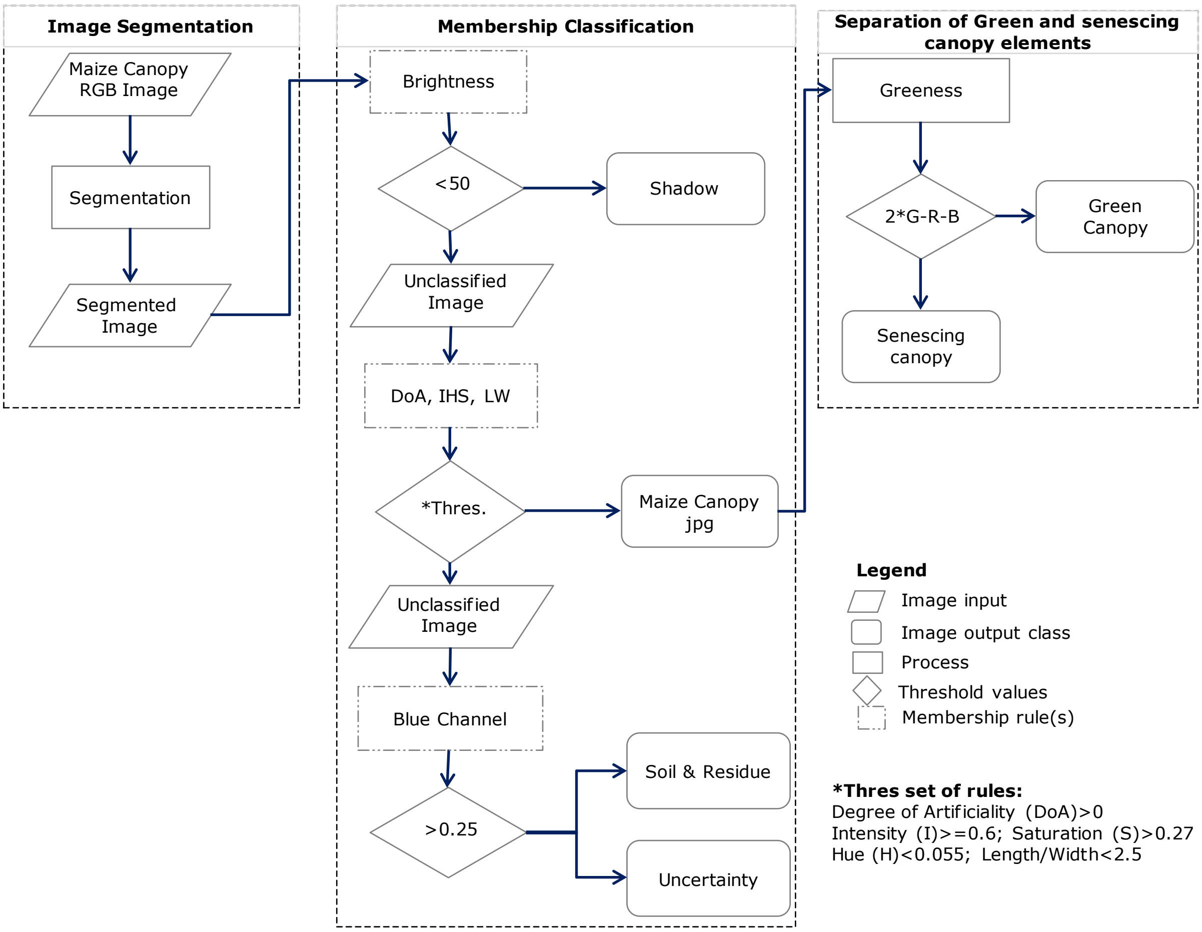

Figure 10. Image Classification Flow chart.

Colour space models have been used in several studies to classify image objects, and in several cases vegetation canopies from their background objects. The traditional red, green and blue (RGB) colour space has been used in combination with thresholding methods to provide good classification results. Several indices have been reported, however the most widely are the greenness **(Eq. 17)** index because of its ability to separate green vegetation elements from other scene elements like soil and non-green elements (Liu *et al.*, 2010). The equation for greenness is given as follows.

$$2 * G - R - B \qquad \textbf{Eq. 17}$$

In order to separate senescing material from the soil background another RGB colour indices, degree of artificiality (DoA) in combination with IHS colour space indices have been reportedly yielded some good results. The IHS detects all living vegetation (Laliberte *et al.* 2007).

$$DoA = \frac{G-R}{G+R} \qquad \textbf{Eq. 18}$$

In this study a combination of RGB and IHS was integrated in membership classification to separate the whole canopy architecture from residue and soil background.

2.8.1. Segmentation

Prior to classification, maize canopy images were partitioned into homogeneous subunits using the multi-resolution segmentation process in eCognition. The algorithm employs a bottom-up approach which classifies images from pixel to object level and merges them up as long as the local thresholds of homogeneity are not exceeded (Timble, 2014). The thresholds are based on three parameters namely scale, shape and compactness of the image. On one hand, scale parameter determines the relative size of the segmented image object, hence imposing control its maximum allowable heterogeneity. On the other hand shape has a linear relationship with colour, decreasing it increases the weight of influence of spectral values on the image. Nevertheless compactness distinguishes compact object in the neighbourhood of less compact ones. In light of the above, an optimum scale of 23 was computed using the ESP tool, to determine the size of image objects to be segmented (Drăguţ *et al.*, 2010). A shape value of 0.1 to maximize on the spectral values of the canopy elements whilst compactness was set at 0.5, to maintain balance between with smoothness (Laliberte *et al.*, 2007).

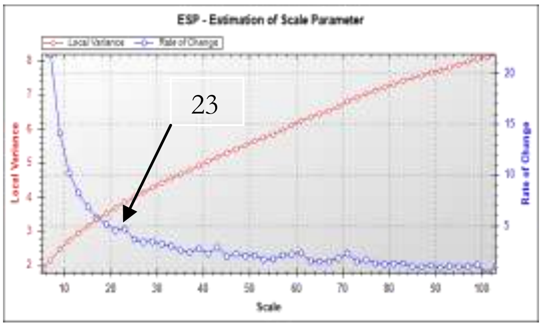

Figure 11. Image segmentation process.
a) *calculation of an appropriate scale* ***b)*** *image segmentation using the scale*

2.8.2. Membership Classification

Membership classification is based on fuzzy logic theory and user defined rules (Benz *et al.*, 2004, Bauer & Strauss, 2014), hence it was used for more easier classifications of images into *shadow, maize canopy and soil-background*. These out classes can be defined using both geometric and spectral characteristics of image objects. The method involves setting rules and thresholds using the "Feature View" tool to define an image object class.

Starting by classifying highly contrasting and unique classes is an easy approach to solve the puzzle of allocating image objects into homogenous groups. In this view, the shadow class, defined by a brightness threshold of less than fifty (<55) was classified first. This was followed by classifying the maize canopy that had a higher level of homogeneity due to the dominant green colour. The degree of artificiality (DoA>0), which tested positive for all living green canopy elements was used along with IHS colour space values: I>=0.6 and S>0.4 which also tested positive to senescing canopy elements, together making the maize canopy class. However this combination of rules misclassified partly misclassified some dry tree leaf residues on the soil surface. A combination of the hue, which tested less positive for dry tree, leaves (H<0.055), and a geometric parameter of leaves, length to width ratio, which is lower in round tree leaves (LW<2.5), than lengthy maize leaves. At this point the bulky of the remaining unclassified image objects were soil and residue, which was classified as soil background. However, to assess the level of uncertainty in the classification, a rule set was defined for soil background class that tested more positive in the blue channel (b>=0.25) of the RGB than the maize canopy elements class.

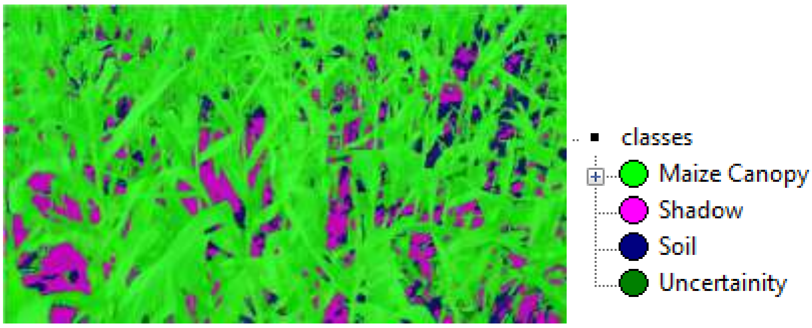

Figure 12. Maize canopy separated from soil background

2.8.3. Separation of Green and Senescing Canopy Elements

After the separation of maize canopy from soil background, a customized object feature was created using **Eq. 17** from the single RBG channels in the feature view space. A greenness threshold was defined at (>0.05) with its inverted direction used as a threshold for senescing canopy elements. As a result two separate classes, green and senescing were created as shown in **Figure 12** below. These two classes were exported separately as (*.jpg*) files with all other classes merged together into one (**Figure 8)**.

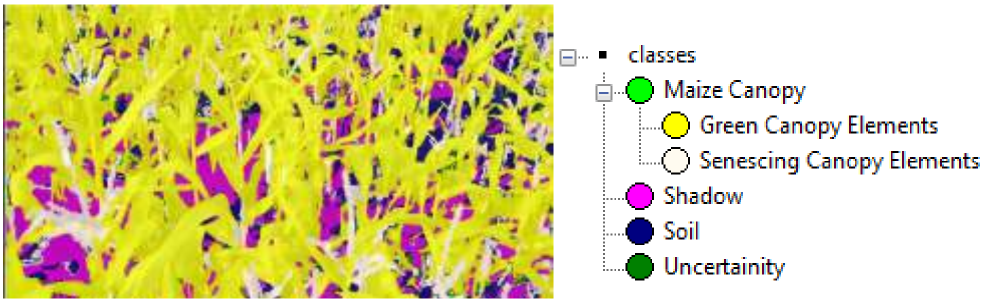

Figure 13. Green canopy separated from senescing canopy elements.

2.9. Binarisation

The binarisation process was completed in CAN-EYE (Weiss, 2013) which can be obtained from http://www6.paca.inra.fr/can-eye (last accessed: 9th September 2013). to extract gap fraction, LAI_{true}, and LAI_{eff}.. The green and senescing images were exported in *.jpg* format separately with other combined into one classes as gap **Figure 8**. The extraction of canopy parameters was accomplished using the **RGB-downward** option for images taken above the canopy as prescribed in the CAN-EYE manual (Weiss, 2012). It allows processing of already classified and unbinarised images, i.e. classified images with their original size.

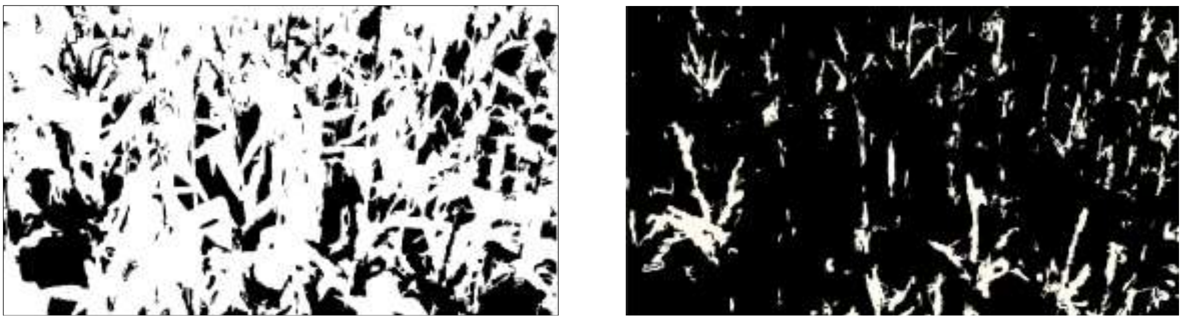

a) **b)**

Figure 14 Green and Senescing images used in CAN-EYE.

2.10. Data Analysis Methods

2.10.1. Data Exploration methods

Data exploration was performed to determine an appropriate statistical method to use: parametric or nonparametric analysis. A Shapiro Wilkins' test was used to quantitatively tested data for normality whilst normal probability plots (Q-Q) were used to qualitatively check for linearity. Nevertheless homogeneity of variance test were used to test for equality of variance whenever an ANNOVA or student's *t*-test was used. However outliers were identified using the box plots and corrected using the winsorizing method.

2.10.2. Testing Smartphone VZA estimation

The $VZA_{smartphone}$ was tested against the $VZA_{inclinometer}$ using Ordinary Least Square Regression (OLSR) model in SPSS (v.16). Fifty synchronised observations between the VZA 50^o to 60^o were selected from four randomly selected excel files each and averaged . Therefore, each excel file represented a replicate of each observation selected. An ordinary least square regression (OLSR) model was then used to compute the residuals to calculate RMSE from **Eq 19** below.

$$RMSE = \sqrt{\frac{\sum {e_i}^2}{n}} \qquad \textbf{Eq 19}$$

where e_i is the residual or error at the i^{th} observation and **n** is the total number of observations in the VZA direction per sample.

2.10.3. LAI Sensitivity Analysis

A sensitivity test was preformed across the VZA bins. The mean LAI_{true} values were computed for 50 observations per bin assuming normal distribution of data. Scatter plots were then plotted from these average values to qualitatively assess the sensitivity of LAI_{true} with varying VZA. Furthermore, sensitivity analysis index for LAI $(\mathrm{LAI_S})$ was also computed using the Ordinary Least Square Regression (OLSR) method and the general linear model is given below.

$$y = b_o + b_1 x \qquad \textbf{Eq 20}$$

where y is the average LAI_{true} for each bin, **x** is the VZA intercept and $\mathbf{b_1}$ the gradient of the model. The variation in LAI_{true} in the VZA direction was then tested using the, coefficient of determination **(R^2)** and the root mean square error **(RMSE) of the** averages assuming normally distributed data**.** The sensitivity of LAI_{true} due to the variation in errors in the VZA was then evaluated using the equation below:

$$\mathrm{LAI_S} = \frac{\mathrm{b1}}{RMSE}$$ (Gonsamo & Pellikka, 2012; Cao *et al.*., 2014). **Eq 21**

where LAI_s of the i^{th} observation is equal to ***t*,** the student ***t***-test statistic.

2.10.4. Senescence effect on LAI

The LAI_{true} and senescing canopy indices were added together to give LAI_{canopy}. An independent student *t*-test was then used to compare between the means of LAI_{canopy} and LAI_{true} to test whether there is a significance difference between the two. In essence, gap fraction theory increases when senescing material is removed from the LAI_{canopy} , leading to a decrease in LAI_{true}, assuming canopy elements are black foliage. The testing of equality of variances was done a prior to determine appropriate degrees of freedom for the *t*-test

2.10.5. Validation of Classification

Image classification was validated using an independent student *t*-test. The mean of a total of 500 observations from classified images were tested against the mean of 50 observations from direct measurements at 95% significance level, for both LAI_{true} and senescence.

3. RESULTS AND DISCUSSION

3.1. Sample characteristics

A Shapiro-Wilk's test ($p>0.05$), skewness between -0.35 and -0.03 (std error = 0.34) and kurtosis between -0.79 to -0.28 (std error = 0.66) for both $VZA_{smartphone}$ and $VZA_{inclinometer}$, showed that all the variables approximated normal distribution. Furthermore, a visual inspection of their histograms, normal Q-Q plots and box plots supported these outcomes.

3.2. Estimating VZA using Smartphone

3.2.1. Testing smartphone on a platform

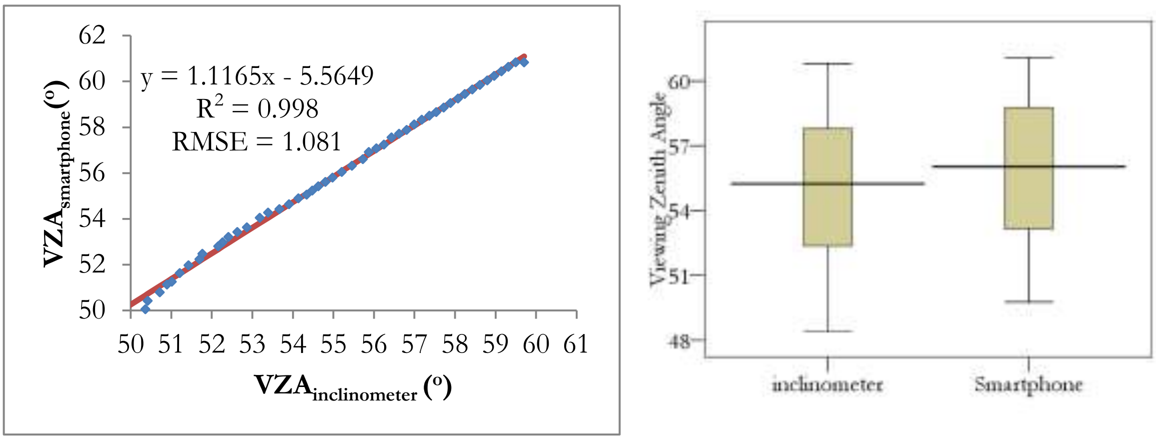

Figure 15a) A linear regression model, **b)** Boxplots for $VZA_{smartphone}$ vs $VZA_{inclinometer}$.

A regression model of 50 VZA observations averaged over 4 replicates from both smartphone and inclinometer were plotted. There was a high correlation (R^2 = 0.998, RMSE = 1.081) between the two measurements **(figure 15a)**. We therefore failed to reject the null hypothesis and concluded that the RMSE between $VZA_{smartphone}$ and $VZA_{inclinometer}$ is greater zero (RMSE>0). The large RMSE was due to offsets that were observed at the start of the model, around 50° to. This was caused by the instability of the platform due to the deceleration of speed (m/s) around this region **(figure 8).** The measurements that were recorded at the start and end of this region had noise pattern of peaks and drops that resulted a in large RMSE. However a good fit was observed starting from the VZA 53°, when the speed was more stable. The noise around 60° was reduced due a continuous steady constant speed that was maintain before rolling back the platform to the starting position. Interestingly, the $VZA_{inclinometer}$ observations were at least 1° less than $VZA_{smartphone}$ at the start of the recording as shown in **(figure 15b).** This also explains noise of the data at the initial VZA bins. It can be clearly seen that eventually these offsets of the start VZA bins resulted in the differences the two measurements.

The high coefficient of determination (R^2 = 0.998) between the two measurements explicitly reveals the success rate of the synchronisation process. An Independent student t test confirmed that there was no significance difference ($P>0.05$) between the $VZA_{smartphone}$ and $VZA_{inclinometer}$ assuming equality of variance ($P>0.05$). The success rate of the synchronisation process which used time as an identifier of individual VZA observations, was firstly accomplished through proper device time correction using the GPS time application from (play.google.com/store/apps), as the first line of accuracy (**figure 16**). The time difference of less than five seconds (<0.5 sec), ensured that all the VZA measurements were brought to the same time scale for a synchronisation with 100% overlap of the region of interest (ROI).

Figure 16. Smartphone device time correction.

	$VZA_{inclinometer}$	$VZA_{smartphone}$
t-statistic	0.536	1.064
DF	248	248
P(T<=t)	0.593	0.288

Table 2. Validation of synchronisation

Lastly, comparability between the measurements was made possible through the degree of accuracy of the VZA devices: digital inclinometer, resolution of 0.1° and accuracy of ±0.2° (http://www.wixey.com) and smartphone motion sensor as illustrated in **(figure 5a)**.

3.2.2. Testing smartphone by hand

From the result in **figure 15b**, which shows that a smartphone motion sensor is more reliable than inclinometer, an attempt was made to test the accuracy of a smartphone by estimating the VZA 57.5° separately. A sample size of 300 observations were recorded five times and average VZA were computed (**table 3**). The standard errors from 0.012 to 0.023 were due to the instability of the hand during recording. It is important to note that smartphone motion sensor is highly sensitive to very small external forces exerted on the phone resulting the deviations from the target VZA. The highest range was 0.71 in the first test and lowest 0.59 in the third test. This demonstrated that a smartphone can estimate the VZA with minimum errors. Hence the source of errors introduced in previous section could be from the platform or inclinometer.

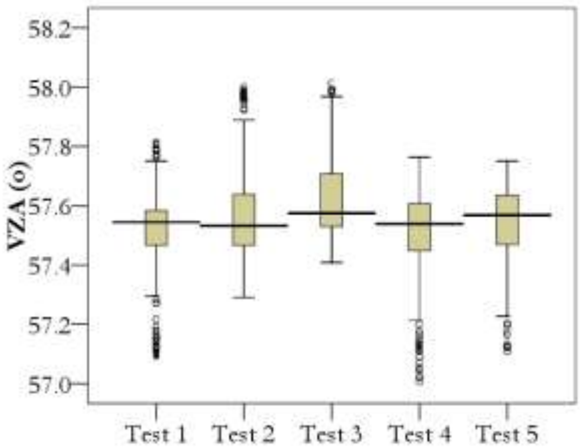

Figure 17. Box plot for estimation of VZA 57.5°

Statistic	**Test 1**	**Test 2**	**Test 3**	**Test 4**	**Test 5**
N	300	300	300	300	300
Mean	57.52	57.5	57.6	57.5	57.5
std Error	0.012	0.022	0.02	0.023	0.02
Maximum	57.8	57.9	58	57.8	57.8
Minimum	57.09	57.29	57.41	57.01	57.1

Table 3. Summary statistics for estimation of VZA 57.5°

3.3. LAI Sensitivity

Average LAI_{true} values were computed from 50 normally distributed observations for ten bins each. A sensitivity analysis of LAI_{true} to unsteady VZA was performed using OLSR model and scatter plots of the means. A strong correlation between LAI_{true} and VZA- Error was observed for $VZA_{smartphone}$ (R^2=0.96, RMSE=0.01). However, the RMSE (0.01) was below 5% reported by Baret *et al.*, (2010) from a Poisson distribution model only at 57.5° VZA (**Eq 4**). This result was least expected since in this study since varying VZA was supposed to increase error in the estimation of LAI_{true}. Instead the errors remained the same as reported from the theoretical study performed at 57.5°. This can be explained by the relationship between the LAI_{true} and the G-function which also varies with VZA, as described in (**Eq 6).** The G-function in the VZA 50°-60° region is close to 0.5 and invariant at 57.7° (G = 0.5). At the same time cos θ_v which describes the path length through which light pass in a canopy decrease marginally with increasing VZA. As a result, there is a very small change in LAI_{true} with respect to varying VZA**.** This can also support the idea of restricted field of view of 10° ($\pm$ 5°) when taking photographs around the VZA 57.5° reported by Baret *et al.*, 2010; and Liu *et al.*, (2013b). This method has been so attractive not only in getting the VZA angle correct but also is increasing the resolution of the photographs which helps to distinguish green from senescence.

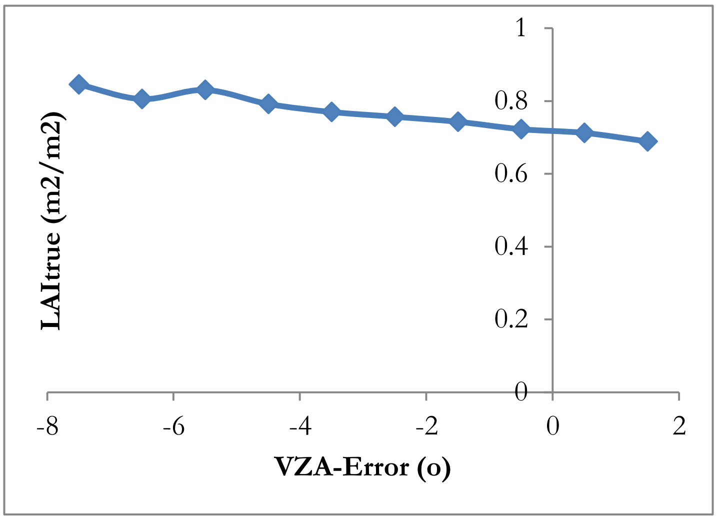

Figure 18. The sensitivity analysis line scatter plot for smartphone

N	10
RMSE	0.01
b_1	-0.017
LAI_s	-1.72
P(T<=t)	-13.95
R^2	0.96

Table 4. Sensitivity analysis statistics for smartphone

The sensitivity (LAI_s) were evaluated using **Eq. 21** and the results are shown in **table 3**. below. This result shows that sensitivity of LAI_{true} (LAI_s = -1.72) was significant to the variation in VZA (LAI_s >-13.95) for the smartphone. The magnitude of the sensitivity is partly caused by both a less steep slope of the regression model (b_1 = -0.017). The bigger the slope the more sensitive the LAI_{true} and vice versa. The size and direction of the slope is explained by the relationship between the G-function (G) and VZA as shown in **(figure 1).** The G-function is in turn directly depended on the average leaf angle (ALA) distribution of the canopy in a direction perpendicular to the normal plane (Wilson, 1963; Chen & Black, 1991). However, the ALA of the canopy is also influenced by the crop phenological stage (Monteith, 1969). Leaf angle distributions functions tend to converge at 57.5°, when G=0.5. When G>0.5 the gradient of the leaf angle distributions tend to be negative whilst when G<0.5 the gradient is positive (Myneni *et al.*, 1989; Ross, 1981). Hence prior knowledge of the G-function of a particular canopy archetype helps to explain the direction of sensitivity of that canopy with varying VZA.

The G-function of maize was measured by (Fang, 2015), in parallel study and the results are given in (**figure 19)** below (in broken line). It can be seen that the G-function of maize is above G = 0.5 and hence it has a negative gradient which agrees with regression model result in **table 4.** More interestingly, Liu *et al.*, (2013) also reported an average ALA for corn of 48.2° $\pm$ 8° over two growing seasons which is greater than ALA for spherical distribution (ALA =45°), hence G>0.5.

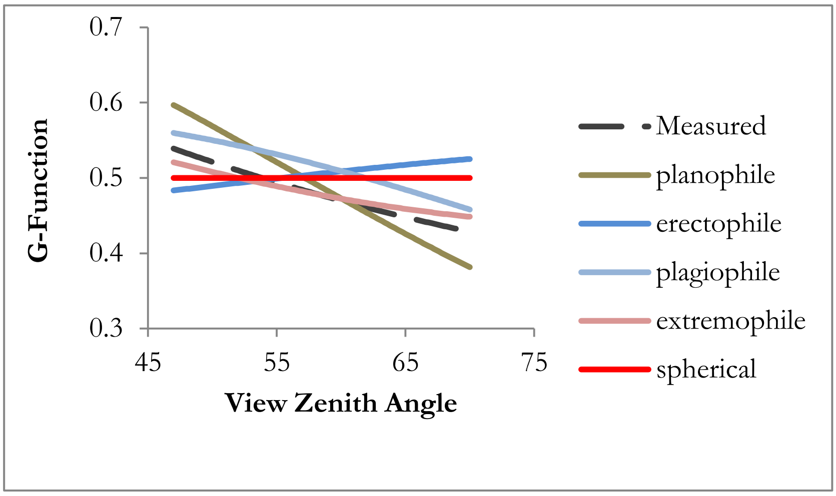

Figure 19. The sensitivity of the G-function with varying VZA
(source Fang, 2015)

3.4. Effect of Senescing Canopy Material on LAI

3.4.1. Sample characteristics for LAI_{true},

	N	Mean	Std Deviation	Std Error Mean
LAI_{true} Smartphone	500	1.228	0.397	0.018
$Senescence_{smartphone}$	500	0.249	0.035	0.002
LAI_{canopy} smartphone	500	1.47	0.403	0.018

Table 5. Summary of smartphone canopy variables, LAI_{true}, Senescence and LAI_{canopy}.

A total of 500 observations across VZA bins was used to calculate LAI_{canopy} values for smartphone measurements. LAI_{canopy} values were calculated by adding green and senescing canopy elements measurements together. A student t-test was then used to test for equality of means between LAI_{canopy} anLAI_{true} to assess the effect of removal of senescing material from LAI_{canopy} A summary table below describes all the variables that were used to computed LAI_{canopy} values.

3.4.2. Test for Equality of between Means LAI_{canopy} and LAI_{true}

	Test for Equality of Variances		***t*-test for Equality of Means**		
	F	significance	t-test	df	P(T<=t)
Smartphone	0.089	0.765	15.203	498	p<0.001

Table 6. Testing for equality of means between LAI_{true} and LAI_{canopy} for smartphone

The test for equality of variances showed that there is a significance difference (P<0.001) between the means of LAI_{true} and LAI_{total}. We therefore rejected the null hypothesis in favour of the alternative hypothesis and concluded that there was a significant decrease in the LAI_{true} when senescing canopy material is removed from LAI_{total} assuming has black canopy foliage. This is because gap fraction measurements from which LAI was estimated (**Eq 4.**) are very sensitive to green and non-green canopy materials (Baret *et al.*, 2010). The effect of senescing elements on LAI estimation using LAI 2000 was reported by Liu, (2010). The instrument tends to overestimate LAI because it measure both green and senescence. In another study by Liu *et al.*, (2013), the effect of non-green due to stem elongation in wheat resulted in a very week correlation when compared to direct measurements. Conversely other crops like maize and soya beans which had completely green canopies had a strong correlation with direct measurements.

When the proportion of senescing elements were quantified, it was observed that the canopy had only 16.95% from both smartphone measurements. More interestingly the minimum threshold of non-green elements which can result in significant decrease can be lower than these observed values. It is therefore important to note that separation of green from senescing elements is also a very important step towards accurate estimation of LAI_{true} from gap fraction measurements.

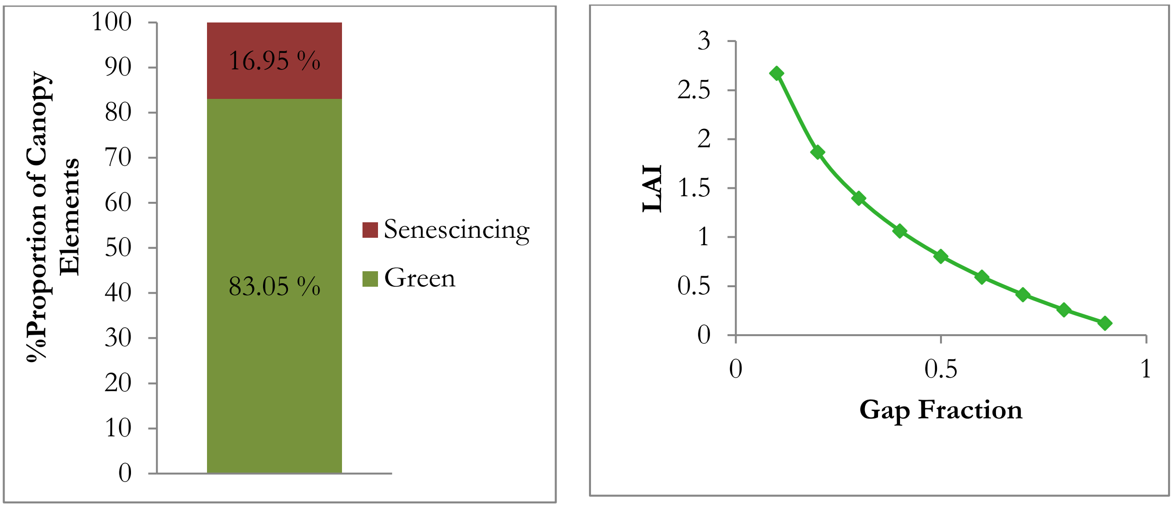

Figure 20 a. The percent proportions of canopy elements **b)** sensitivity of LAI to gap fraction.

3.5. Validation of Classification

The accuracy of classification method was tested using an independent student t-test method. Validation was done for LAI_{true} and senescence variables which were classified in eCognition and the results are given below.

	Test of Equality of Variance		t-test of equality of means			
	F	sig	df	Mean square	P(T<=t)Sig	
LAI_{true} Inclinometer	2.794	0.097	548	0.052	0.853	0.936
LAI_{true} smartphone	2.752	0.098	548	0.049	0.918	0.982
$Senescence_{inclinometer}$	6.073	0.014	84.6	0.001	0.676	0.725
$Senescence_{inclinometer}$	5.360	0.021	77.8	0.004	0.528	0.045

Table 7. Validation of image classification

There was no significant difference (P>= 0.05) between the direct measurements and estimated measurements from photographic methods assuming equality of variance (P>=0.05) for LAI_{true} measurements and no equality of variance for senescence measurements (P<=0.05). The LAI_{true} measurements had better agreement with the direct measurements because the green canopy material was much easier to distinguish and separate from other classes. Greenness of the canopy was classified using **Eq 17.** which exhibits high spectral contrast between reflected radiation of green leaves and other surrounding elements like soil and senescing material (Liu *et al.*, 2010). Classification of shadow was done a priori to avoid the confusion of misclassification between senescing canopy material and green (Bauer &

Strauss, 2014). Unfortunately some of the green elements under the shade were misclassified as shadow due to their brightness levels below threshold. This problem caused a lot of impact on the classification of senescing because most of the non-green canopy material were in the shade. That is why the p-values for senescing canopy were lower than for green which had its greater proportion of the outside the shade. Nevertheless the senescing canopy material were also significant because of the combination of IHS with RGB colour spaces. The two colour spaces are more effective than RGB alone, because of the high correlation between the G and R channels which makes it difficult to distinguish green and senescing canopy material (Laliberte *et al.*, 2007). The intensity and saturation effectively isolated all canopy elements. Although some non-green residuals on the soil surface were also classified, geometric membership functions were used to isolate them from the canopy elements. This was effective because the senescing maize elements were slander in shape and longer in size when compared to the dry tree leaves which more circular in shape.

4. CONCLUSIONS AND RECOMMENDATION

The purpose of this study was to evaluate the possibility of improving of LAI estimation by a measuring view zenith angle (VZA) correctly and assessing whether the use of a smartphone motion sensor can be used to improve its estimation. In-order to accomplish this, the study therefore tested the capability of a smartphone motion sensor technique against a digital inclinometer device on VZA measurements. The smartphone and inclinometer VZA measurements were strongly correlated (R^2=0.998, RMSE=1.081). Although the null hypothesis could not be rejected, there was only a small difference (RMSE = 1.081°) between smartphone and inclinometer VZA measurements. The measurements were done on the same platform for easy comparability, there were uncertainties at every step of measurement as described in the methods. Unfortunately the cumulative effect of these uncertainties at each step increased the error margin between the two measurements. However, when the smartphone motion sensor was tested by hand the average VZA was 57.5° in four out five test with small standard errors ranging from 0.012 to 0.023. Therefore the source of the errors between the smartphone and inclinometer VZA measurements could be from the platform of inclinometer.

In-order to put the applicability of a smartphone into context, the study also tested the sensitivity of LAI_{true} (LAI_s) to varying VZA given that LAIs is equal to the *t*-test statistic **(Eq. 21)** The sensitivity of LAI_{true} (LAI_s = -1.72) to varying VZA was significant (LAIs > -13.95). The RMSE of LAI_{true} due varying VZA was also compared against a theoretical value of 5% when VZA errors are smaller than 2° around the 57.5°, as reported by Baret *et al.*, (2010). Surprisingly the RMSE for estimating LAI_{true} was in agreement with the theoretical one (R^2=0.96 RMSE<0.05), with the variation around the VZA 57.5° was less than 2°. It was noted that, perhaps this was due to the proximity of the G-function in the VZA 50° to 60° to (G = 0.5). The same explanation also applied for low sensitivity of LAI_{true}. Furthermore, the negative gradient of the sensitivity was attributed to the leaf angle distribution of maize whose G-function (G>0.5), hence converges at VZA 57.5° with a negative gradient. As a result a conclusion was drawn that the sensitivity of LAI_{true} to varying VZA is negative and small as reported in earlier studies (Myneni *et al.*, 1989; Ross, 1981).

Furthermore, the study also examined the sensitivity of LAI_{true} to the removal of senescing canopy material. A new variable LAI_{canopy} was computed by inferring from LAI_{true} and senescence. The study demonstrated that there was a significant difference (P<0.001) between LAI_{canopy} and LAI_{true}, which explains the effect of removal of senescing material assuming that the canopy is a black foliage. Hence it was concluded that removal of senescing canopy elements can play an important role in accurate estimation of LAI_{true}. However, the results were going to be more informative if data for different crop stages were collected using both bottom-looking-up and top-looking-down approaches. The canopy elements at the bottom are usually difficult to capture using the top-looking-down approach because they are covered and usually under shade. This resulted in underestimation of the senescing canopy elements. However the top-looking-up approach tends to capture the whole canopy from the bottom to the top. Hence, implementing the two methods together will therefore help to adequately answer the question on both sensitivity of LAI to varying VZA and removal of senescence from total canopy elements.

The accuracy of the classification of images was validated against direct measurements using an independent student *t*-test. A good agreement (P>0.05) between LAI_{true} measurements and the direct measurements was confirmed assuming equality of variance (P>0.05) of individual observations. This was attributed to a more accurate classification of green canopy elements class. However the senescing canopy elements class demonstrated a good agreement (P>0.05) with direct measurements but assuming unequal variances ($P<0.05$). This was explained by misclassification errors on senescing canopy materials to the effect of shade on the bottom canopy elements.

4.1.1. Recommendations

Smartphone motion sensor fusion is quite promising to measure the attitude information of a smartphone. LAI from gap fraction measurements. However their full potential can only be realized when all its accessories relevant for improving photographic measurements are exploited via a application (app.). Hence an application implementing a camera sensor to capture the canopy, GUI to control the camera sensor, and increased memory to store the data should be developed and tested against the conventional photographic methods. VZA obtained through MSF can therefore be considered a suitable trigger to fire the camera sensor in an effort to minimize operator-related errors in obtaining canopy photos at 57.5^{o}. Furthermore, the app. should also have a self-contained image processing functionality implementing both thresholds methods and RGB colour space to enable users to instantly and accurately obtain LAI measurements. The software GUI can be enhance to control the processing functionality embedded in the app, as such images are acquired and processed at the same time. In addition, images can be brought to scale by measuring and object of a known scale by the same application. This helps to minimize accumulation of errors that are obtained when a chain of methods and software are used to acquire and process images as the case of this study.

With regards to senescence, a similar study should also be undertaken with crops at different levels of senescence using both top-looking-down and bottom-looking-up approach. In this study data was collected from a crop at one level of senescence by virtue of its crops stage. Use of different levels of senescence helps to reveal the extent to which removal of senescence has on LAI estimation. In some studies canopies with very low amounts of senescing elements are assumed to be green, yet the critical threshold amount of senescing material is not known. I such cases, the estimation of LAI may be erroneous when a homogeneously green canopy is assumed.

LIST OF REFERENCES

Baret, F., De Solan, B., Lopez-Lozano, R., Ma, K., & Weiss, M. (2010). GAI estimates of row crops from downward looking digital photos taken perpendicular to rows at 57.5° zenith angle: Theoretical considerations based on 3D architecture models and application to wheat crops. *Agricultural and Forest Meteorology*, *150*(11), 1393–1401. doi:10.1016/j.agrformet.2010.04.011

Bauer, T., & Strauss, P. (2014). A rule-based image analysis approach for calculating residues and vegetation cover under field conditions. *CATENA*, *113*, 363–369. doi:10.1016/j.catena.2013.08.022

Benz, U. C., Hofmann, P., Willhauck, G., Lingenfelder, I., & Heynen, M. (2004). Multi-resolution, object-oriented fuzzy analysis of remote sensing data for GIS-ready information. *ISPRS Journal of Photogrammetry and Remote Sensing*, *58*(3-4), 239–258. doi:10.1016/j.isprsjprs.2003.10.002

Bréda, N. J. J. (2003). Ground-based measurements of leaf area index: a review of methods, instruments and current controversies. *Journal of Experimental Botany*, *54*(392), 2403–17. doi:10.1093/jxb/erg263

Bréda, N. J. J. (2003). Ground-based measurements of leaf area index: a review of methods, instruments and current controversies. *Journal of Experimental Botany*, *54*(392), 2403–17. doi:10.1093/jxb/erg263

Cao, J., Gu, Z., Xu, J., Duan, Y., Liu, Y., Liu, Y., & Li, D. (2014). Sensitivity analysis for leaf area index (LAI) estimation from CHRIS/PROBA data. *Frontiers of Earth Science*, *8*(3), 405–413. doi:10.1007/s11707-014-0432-0

Cellina, F., Anna, F., Rivola, D., Pampuri, L., Rudel, R., & Rizzoli, A. E. (2013). Using Smartphones to Profile Mobility Patterns in a Living Lab for the Transition to E-mobility (pp. 154–163).

Chen, J. M., & Black, T. A. (1991). Measuring leaf area index of plant canopies with branch architecture. *Agricultural and Forest Meteorology*, *57*(1-3), 1–12. doi:10.1016/0168-1923(91)90074-Z

Chen, J. M., & Cihlar, J. (1995). Quantifying the effect of canopy architecture on optical measurements of leaf area index using two gap size analysis methods. *IEEE Transactions on Geoscience and Remote Sensing*, *33*(3), 777–787. doi:10.1109/36.387593

Confalonieri, R., Foi, M., Casa, R., Aquaro, S., Aquaro, S., Tona, E., Peterle, M., … Acutis, M. (2013). Development of an app for estimating leaf area index using a smartphone. Trueness and precision determination and comparison with other indirect methods. *Computers and Electronics in Agriculture*, *96*, 67–74. doi:10.1016/j.compag.2013.04.019

Demarez, V., Duthoit, S., Baret, F., Weiss, M., & Dedieu, G. (2008). Estimation of leaf area and clumping indexes of crops with hemispherical photographs. *Agricultural and Forest Meteorology*, *148*(4), 644–655. doi:10.1016/j.agrformet.2007.11.015

Denis Havlik and Gerald Schimak. (2014). State and trends in mobile observation applications. In N. W. T. Q. and A. E. R. (Eds. . Daniel P. Ames (Ed.), *International Environmental Modelling and Software Society (iEMSs)*. San Diego, CA. Retrieved from http://www.iemss.org/sites/iemss2014/papers/iemss2014_submission_388.pdf

Drăguţ, L., Tiede, D., & Levick, S. R. (2010). ESP: a tool to estimate scale parameter for multiresolution image segmentation of remotely sensed data. *International Journal of Geographical Information Science*, *24*(6), 859–871. doi:10.1080/13658810903174803

DVDVideoSoft. (n.d.). *FREE Video & DVD Software: Download free Video to JPG Converter - make snapshots from video files*. Retrieved January 16, 2015, from http://www.dvdvideosoft.com/products/dvd/Free-Video-to-JPG-Converter.htm

Ebay. (2014). *Do You Need a Digital Camera and a Smartphone? | eBay*. Retrieved August 13, 2014, from http://www.ebay.com/gds/Do-You-Need-a-Digital-Camera-and-a-Smartphone-/10000000177628249/g.html

Francone, C., Pagani, V., Foi, M., Cappelli, G., & Confalonieri, R. (2014). Field Crops Research Comparison of leaf area index estimates by ceptometer and PocketLAI smart app in canopies with different structures ☆. *Field Crops Research*, *155*, 38–41. doi:10.1016/j.fcr.2013.09.024

Gonsamo, A., & Pellikka, P. (2012). The sensitivity based estimation of leaf area index from spectral vegetation indices. *ISPRS Journal of Photogrammetry and Remote Sensing*, *70*, 15–25. doi:10.1016/j.isprsjprs.2012.03.009

Imaging, R. D. (2011). *Cameraphones Are Getting Better, but Do They Really Compare to Cameras? : Page 1 of 2 :*. Retrieved August 13, 2014, from http://www.direporter.com/article/cameraphones-are-getting-better-but-do-they-really-compare-cameras/1

Jonckheere, I., Fleck, S., Nackaerts, K., Muys, B., Coppin, P., Weiss, M., & Baret, F. (2004). Review of methods for in situ leaf area index determination. *Agricultural and Forest Meteorology*, *121*(1-2), 19–35. doi:10.1016/j.agrformet.2003.08.027

Laliberte, A. S., Rango, A., Herrick, J. E., Fredrickson, E. L., & Burkett, L. (2007). An object-based image analysis approach for determining fractional cover of senescent and green vegetation with digital plot photography. *Journal of Arid Environments*, *69*(1), 1–14. doi:10.1016/j.jaridenv.2006.08.016

Liu, J., & Pattey, E. (2010). Retrieval of leaf area index from top-of-canopy digital photography over agricultural crops. *Agricultural and Forest Meteorology*, *150*(11), 1485–1490. doi:10.1016/j.agrformet.2010.08.002

Liu, J., Pattey, E., & Admiral, S. (2013a). Agricultural and Forest Meteorology Assessment of in situ crop LAI measurement using unidirectional view digital photography. *Agricultural and Forest Meteorology*, *169*, 25–34. doi:10.1016/j.agrformet.2012.10.009

Liu, J., Pattey, E., & Admiral, S. (2013b). Assessment of in situ crop LAI measurement using unidirectional view digital photography. *Agricultural and Forest Meteorology*, *169*, 25–34. doi:10.1016/j.agrformet.2012.10.009

Monteith, J. Light Interception and Radiative Exchange in Crop Stands, Agronomy & Horticulture -- Faculty Publications (1969). Retrieved from http://digitalcommons.unl.edu/agronomyfacpub/185

Motion Sensors | Android Developers. (n.d.). Retrieved January 24, 2015, from http://developer.android.com/guide/topics/sensors/sensors_motion.html

Myneni, R. B., Ross, J., & Asrar, G. (1989). A review on the theory of photon transport in leaf canopies. *Agricultural and Forest Meteorology*, *45*(1-2), 1–153. doi:10.1016/0168-1923(89)90002-6

Nackaerts, K., Coppin, P., Muys, B., & Hermy, M. (2000). Sampling methodology for LAI measurements with LAI-2000 in small forest stands. *Agricultural and Forest Meteorology*, *101*(4), 247–250. doi:10.1016/S0168-1923(00)00090-3

Nilson, T. (1971). A theoretical analysis of the frequency of gaps in plant stands. *Agricultural Meteorology*. Retrieved from http://www.sciencedirect.com/science/article/pii/0002157171900926

Pattey, E., Liu, J., & Admiral, S. (2013). Performance of Unidirectional View Digital Photo to retrieve crop LAI using the GreenCropTracker Leaf Area Index (LAI), 1–26.

Ross, I. (1981). *The radiation regime and architecture of plant stands* (p. 391). Springer Science & Business Media. Retrieved from http://books.google.com/books?id=w6SogqDOa54C&pgis=1

Timble. (2014). *Download Free Trial of eCognition Developer 9.0 | Trimble. Reference Guide book*. Retrieved January 04, 2015, from http://www.ecognition.com/free-trial

Watson, D. J. (1947). Comparative Physiological Studies on the Growth of Field Crops: I. Variation in Net Assimilation Rate and Leaf Area between Species and Varieties, and within and between Years. *Annals of Botany*, *11*, 41–76. Retrieved from aob.oxfordjournals.org/content/11/1.toc

Weiss, M. (2013, July 1). *INRA Science and Impact*. Retrieved August 24, 2014, from http://www6.paca.inra.fr/can-eye/Documentation-Publications/Publications

Weiss, M. (2012). Home. Retrieved from http://www6.paca.inra.fr/can-eye

Weiss, M., Baret, F., Smith, G. J., Jonckheere, I., & Coppin, P. (2004a). Review of methods for in situ leaf area index (LAI) determination. *Agricultural and Forest Meteorology*, *121*(1-2), 37–53. doi:10.1016/j.agrformet.2003.08.001

Weiss, M., Baret, F., Smith, G. J., Jonckheere, I., & Coppin, P. (2004b). Review of methods for in situ leaf area index (LAI) determination. *Agricultural and Forest Meteorology*, *121*(1-2), 37–53. doi:10.1016/j.agrformet.2003.08.001

Wilson, J. W. (1960). INCLINED POINT QUADRATS. *New Phytologist*, *59*(1), 1–7. doi:10.1111/j.1469-8137.1960.tb06195.x

Wilson J.W. (1963). Estimation of foliage denseness and foliage angle by inclined point quadrats. *Australian Journal of Botany*, *11*(1), 95. doi:10.1071/BT9630095

5. ANNEXES

5.1. The process tree for image classification

- Separation of Canopy Elements into Green &Senescing
  - Segmentation
    - 23 [shape:0.1 compct.:0.5] creating 'Level1'
  - Membership Classification
    - unclassified with Brightness < 50 at Level1: Shadow
    - unclassified with DoA > 0 at Level1: Maize Canopy
    - unclassified with HSI Transformation Intensity(R=Layer 1,G=Layer 2,B=Layer 3) >= 0.6 at Level1: Maize Canopy
    - unclassified with HSI Transformation Saturation(R=Layer 1,G=Layer 2,B=Layer 3) > 0.4 at Level1: Maize Canopy
    - Maize Canopy with HSI Transformation Hue(R='Layer 1',G='Layer 2',B='Layer 3') < 0.05 and Length\Width < 2 at Level1: unclassified
    - unclassified with b >= 0.25 at Level1: Soil
    - unclassified at Level1: Uncertainity
  - Classification of Green and Non-green
    - 2*G-R-B
      - Maize Canopy with ExG > 0.05 at Level1: Green Canopy Elements
      - Maize Canopy with ExG < 0.05 at Level1: Senescing canopy Elements
  - Export Image Objects
    - all at Level1: export object statistics

5.2. The Shapiro Wilkins Test for Normality

Variable	View Zenith Angle									
	50	51	52	53	54	55	56	57	58	59
LAI $VZA_{Inclinometer}$	0.44	0.31	0.42	0.33	0.71	0.37	0.21	0.55	0.72	0.10
LAI $VZA_{smartphone}$	0.72	0.32	0.42	0.35	0.72	0.37	0.20	0.54	0.54	0.14
Senescence $VZA_{inclinometer}$	0.46	0.22	0.40	0.32	0.11	0.29	0.39	0.83	0.10	0.46
Senescence $VZA_{smartphone}$	0.50	0.29	0.17	0.26	0.11	0.20	0.33	0.54	0.14	0.35

5.3. Skeweness Test for Normality

Variable	View Zenith Angle									
	50	51	52	53	54	55	56	57	58	59
LAI $VZA_{inclinometer}$	-0.21	0.15	-0.22	-0.08	-0.12	-0.80	-0.80	0.53	-0.74	-1.25
LAI $VZA_{smartphone}$	-0.12	0.15	-0.23	-0.09	-0.12	-0.80	-0.82	0.52	0.52	-1.02
Senescence $VZA_{inclinometer}$	0.27	-0.03	0.00	0.40	0.94	-0.72	0.79	0.00	-1.25	0.27
Senescence $VZA_{smartphone}$	0.05	0.34	0.07	0.29	0.80	-0.82	0.69	0.52	-1.02	-0.09

5.4. Kurtosis Test for Normality

Variable	View Zenith Angle									
	50	51	52	53	54	55	56	57	58	59
LAI $VZA_{inclinometer}$	-1.18	-0.86	-1.19	-0.55	-0.44	-0.76	-1.13	-0.45	-0.42	-0.46
LAI $VZA_{smartphone}$	-0.47	-0.84	-1.19	-0.53	-0.47	-0.75	-1.13	-0.47	-0.47	-0.59
Senescence $VZA_{inclinometer}$	-0.77	-1.28	-0.52	-0.68	-0.85	-1.02	-0.45	-0.36	-0.46	-0.77
Senescence $VZA_{smartphone}$	-0.65	-1.07	-1.36	-0.76	-1.01	-1.13	-0.54	-0.47	-0.59	-0.53

5.5. LAI_{true} Box Plots

Inclinometer **Smartphone**

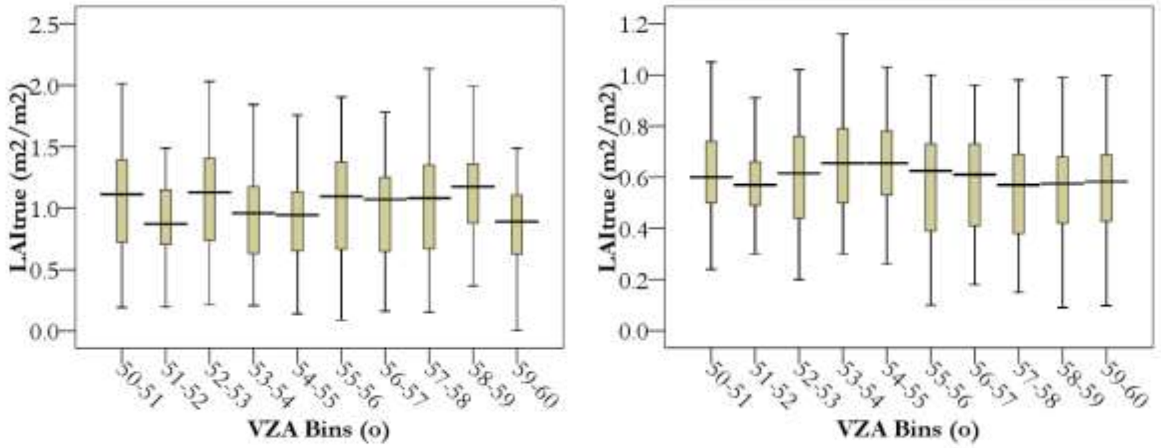

5.6. Senescence Box Plots

Inclinometer **Smartphone**

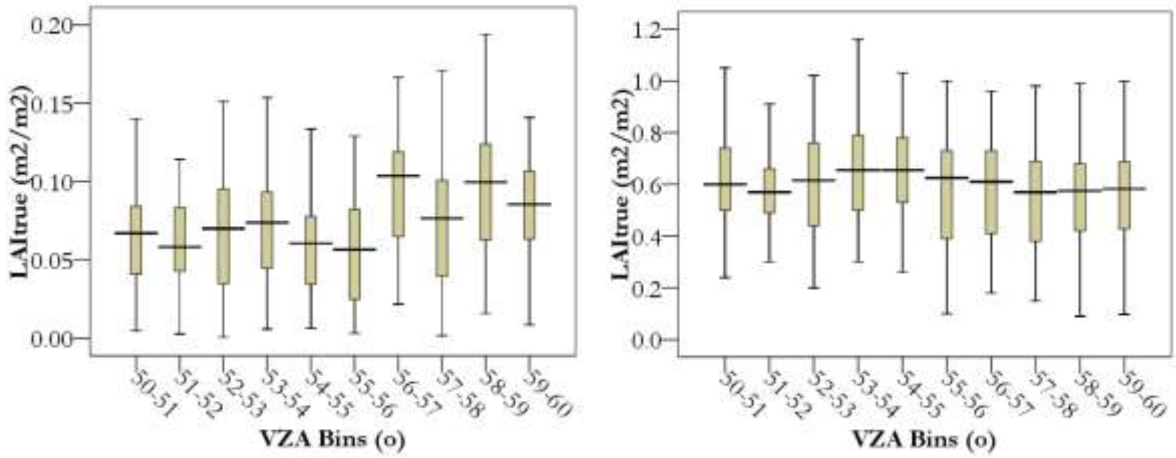

5.7. Probability Plot for smartphone LAI_{true}

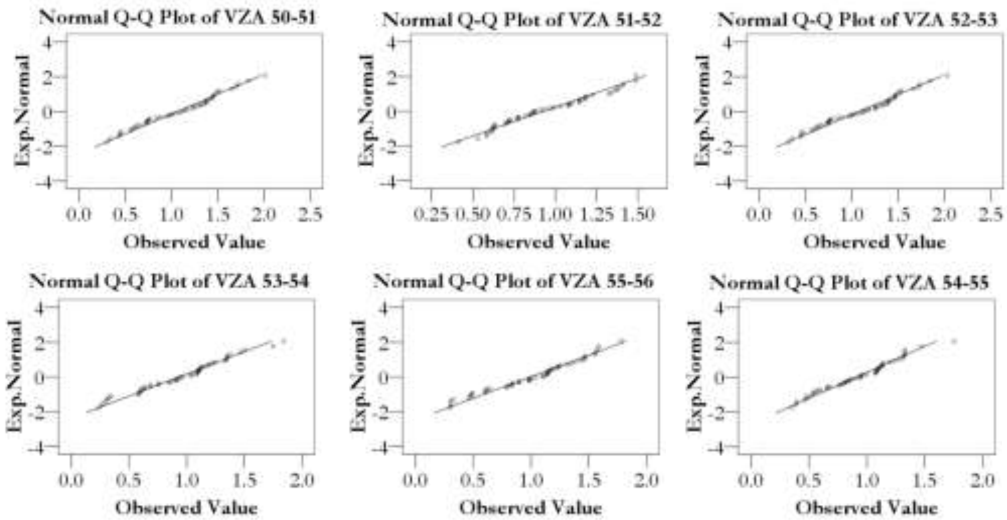

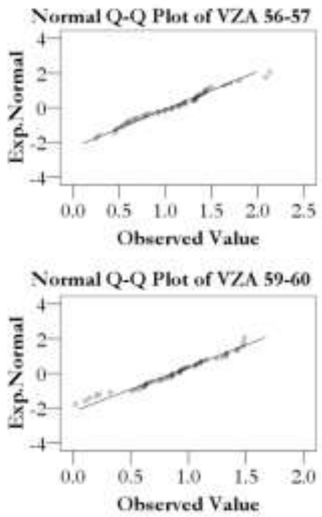

5.8. Normal Probability Plot for Smartphone senescing canopy

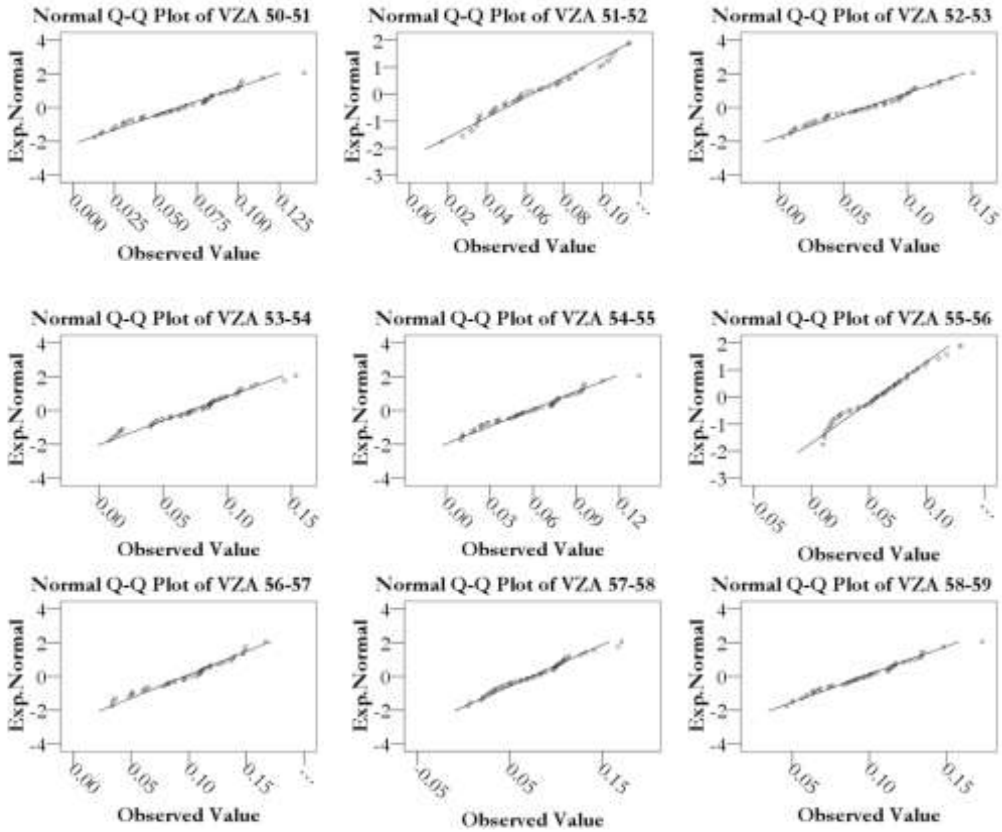

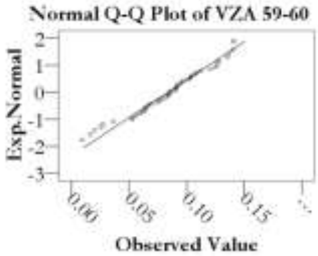
Normal Q-Q Plot of VZA 59-60
Exp.Normal
2
1
0
-1
-2
-3
0.00
0.05
0.10
0.15
Observed Value